Published in final edited form as:
Circ Cardiovasc Imaging. 2009 January ; 2(1): 56–70. doi:10.1161/CIRCIMAGING.108.839092.

Multimodality Cardiovascular Molecular Imaging, Part II

Matthias Nahrendorf, MD, PhD[1,2], **David E. Sosnovik, MD**[2,3], **Brent A. French, PhD**[4], **Filip K. Swirski, PhD**[2], **Frank Bengel, MD**[5], **Mehran M. Sadeghi, MD**[6], **Jonathan R. Lindner, MD**[7], **Joseph C. Wu, MD, PhD**[8], **Dara L. Kraitchman, VMD, PhD**[9], **Zahi A. Fayad, PhD**[10], and **Albert J. Sinusas, MD**[11]

[1] The Centers for Systems Biology, Massachusetts General Hospital and Harvard Medical School, Boston, Mass

[2] Molecular Imaging Research, Massachusetts General Hospital and Harvard Medical School, Boston, Mass

[3] Cardiology Division, Massachusetts General Hospital and Harvard Medical School, Boston, Mass

[4] Department of Biomedical Engineering, University of Virginia, Charlottesville, Va

[5] Radiology and Cardiovascular Nuclear Medicine, Johns Hopkins University School of Medicine, Baltimore, Md

[6] Cardiovascular Molecular Imaging Laboratory, Section of Cardiovascular Medicine, Yale University School of Medicine, and VA Connecticut Healthcare System, New Haven, Conn

[7] Cardiovascular Division, Oregon Health and Science University, Portland, Ore

[8] Departments of Medicine (Cardiology) and Radiology (Molecular Imaging Program at Stanford), Stanford University School of Medicine, Stanford, Calif

[9] Russell H. Morgan Department of Radiology and Radiological Science, The Johns Hopkins University School of Medicine, Baltimore, Md

[10] Translational and Molecular Imaging Institute, Mount Sinai School of Medicine, New York, N.Y

[11] Department of Medicine and Diagnostic Radiology, Yale University School of Medicine, New Haven, Conn

Keywords

molecular imaging; consensus; atherosclerosis; heart failure; myocardial infarction

Molecular imaging has the potential to profoundly impact preclinical research and future clinical cardiovascular care. In Part I of this 2-part consensus article on multimodality cardiovascular molecular imaging, the imaging methodology, evolving imaging technology, and development of novel targeted molecular probes relevant to the developing field of cardiovascular molecular imaging were reviewed.[1] Part II of this consensus article will review the targeted imaging probes available for the identification and evaluation of critical

Correspondence to Matthias Nahrendorf, MD, PhD, MGH-CMIR, 149 13th Street, Charlestown, MA 02129. mnahrendorf@mgh.harvard.edu and Albert J. Sinusas, MD, Yale University School of Medicine, Nuclear Cardiology, 3FMP, PO Box 208017, New Haven, CT 06520-8017. albert.sinusas@yale.edu.
Matthias Nahrendorf and David E. Sosnovik contributed equally to this work.

The opinions expressed in this article are not necessarily those of the authors or of the American Heart Association.

Disclosures
None.

pathophysiological processes in the cardiovascular system. These include novel imaging strategies for the evaluation of inflammation, thrombosis, apoptosis, necrosis, vascular remodeling, and angiogenesis. The current article will also review the role of targeted imaging of a number of cardiovascular diseases, including atherosclerosis, ischemic injury, postinfarction remodeling, and heart failure, as well as the emerging fields of regenerative, genetic, and cell-based therapies. Special emphasis is placed on multimodal imaging, as these hybrid techniques promise to advance the field by combining approaches with complementary strengths and off-setting limitations.[2,3]

Although some applications of molecular imaging are well established, other clinical applications are under development and still emerging, such as early detection of atherosclerosis or unstable plaque.[4] The goals of molecular imaging are to refine risk assessment, facilitate the early diagnosis of disease before the occurrence of debilitating events, aid in the development of personalized therapeutic regimens and to monitor the efficacy of complex therapies. However, to translate the evolving targeted imaging probes, technologies, and applications into clinical care, the imaging community will need to overcome several hurdles. Therefore, the current review will also discuss the opportunities and challenges associated with the implementation and advancement of targeted molecular imaging in clinical practice, and the realization of image-directed personalized medicine.

Critical Pathophysiological Processes

In this initial section, we will review the role of targeted molecular imaging for the evaluation of a number of critical pathophysiological processes of the cardiovascular system.

Inflammation

The chemical and spatiotemporal diversity of inflammatory factors and a growing appreciation of inflammation in cardiovascular disease have engendered interest in targeting the immune system for cardiovascular molecular imaging. Among the prospective targets, proteolytic enzymes and circulating leukocytes have received the most attention. The development of “smart” protease-activatable probes equipped with specific peptide sequences that can be recognized by proteases (ie, cathepsins, matrix metalloproteinases [MMPs]) and that, on enzyme recognition and cleavage, dequench their fluorochromes and fluoresce,[5] has given rise to optical imaging of proteolysis in a number of cardiovascular conditions.[6–8]

Studies investigating the accumulation of leukocytes to tissue reflect directly how inflammation can be targeted for molecular imaging of the inflammatory cascade. A number of ex vivo and in vivo approaches in both atherosclerosis and heart failure have reported sensitive and quantitative imaging of monocyte accumulation to inflammatory sites (Figure 1).[9–11] Naturally phagocytic, these myeloid cells can be labeled easily with optical, nuclear, and superparamagnetic agents for multiscopic, multimodality imaging. Cell trackers such as VT680, a near-infrared reagent that allows for in vivo multiscopic imaging, readily labels leukocytes ex vivo.[12] ^{111}In-oxine, an FDA-approved isotope cell-tracker can report on monocyte accumulation in atherosclerosis and heart failure by autoradiography and single-photon emission computed tomography (SPECT)/computed tomography (CT) imaging.[10,11] For studies in which longer tracking times are needed, stably-transfected fluorescent proteins under control of specific promoters can be used. For example, mice that express green fluorescent protein under the CX_3CR1 promoter have yielded valuable insights into monocyte biology.[13] Collectively, these studies have begun to illuminate the kinetics of cellular infiltration in living animals and thus have provided novel biological insight as well as the possibility for clinical translation. Among the challenges that remain are the high cell turnover rates that dilute signal and prevent long-term imaging, possible activation and cell loss due to ex vivo labeling, the need to discriminate between various myeloid subsets, and the need to

target selectively nonphagocytic leukocytes. As more mechanistic insights of immune mechanisms that govern cardiovascular disease become available through classical and imaging approaches, imaging targets will be identified with the hope to, eventually, image the inflammatory cascade comprehensively at its various stages.

Thrombosis

Thrombosis plays a central role in myocardial infarction, stroke, atrial fibrillation and venous thromboembolism. The potential of molecular imaging in these conditions is 2-fold: (1) to physically detect and diagnose thrombi and (2) to characterize their nature and propensity to respond to anticoagulation and thrombolysis. Strategies to image the central events in thrombus formation including platelet activation,[14] the generation of fibrin,[15] and the cross-linking of fibrin strands by FXIII,[16] have been developed.

Ligands to the glycoprotein II_bIIIa receptor have been conjugated to technetium,[14] and iron-oxide microparticles[17] for SPECT and MRI, respectively. A peptide specific for activated FXIII has been used to image venous thrombosis using fluorescence imaging techniques in vivo.[16] However, the most extensive experience to date in the imaging of thrombosis in vivo has been with EP2104R (Epix Pharmaceuticals, Lexington, Mass) a small gadolinium chelate targeted to fibrin.[18] Studies with EP2104R in rabbits and swine documented the ability of the agent to detect acute and chronic arterial and venous thrombi.[19,20] On the basis of this extensive preclinical experience, 52 patients with suspected thrombosis have now been imaged with this agent.[21] The initial clinical experience with EP2104R shows that the agent is able to successfully detect arterial, venous and intracardiac thombosis in humans (Figure 2). This important experience demonstrates both the feasibility and potential value of targeted cardiovascular molecular MRI in patients.

Apoptosis

Apoptosis plays an important role in diseases of both the myocardium and the vasculature. During ischemia-reperfusion up to 30% of cardiomyocytes (CMs) in the injured myocardium become apoptotic.[22] The level of CM apoptosis in heart failure is significantly lower (<1%) but persists over many months resulting in the net loss of a large number of CMs.[23] The inhibition of apoptosis with caspase-inhibitors in animal models of both ischemia-reperfusion and heart failure is highly cardioprotective.[24–26] Modulation of CM apoptosis thus provides an attractive target for both molecular imaging and therapy of cardiovascular disease.

The hallmark of apoptosis is the activation of the cytoplasmic protease caspase-3. Small molecules, such as isatins, have been labeled with positron-emission tomography (PET) tracers and used to target caspase-3,[27] but the experience with these agents in still very preliminary. A more extensively used approach has been to target the presence of phosphatidylserine on the outer cell membrane of apoptotic cells.[28] Phosphatidylserine is a membrane phospholipid, normally found only on the inner cell membrane, which becomes translocated to the outer cell membrane soon after the activation of caspase-3. Phosphatidylserine on the apoptotic cell membrane has been targeted with Annexin V[25] and the C2 domain of synaptotagmin.[29] Pioneering work with technetium-labeled annexin in humans has shown that cell death in the myocardium can be imaged with this agent in the acute coronary syndromes,[30] heart failure,[31] and transplant rejection.[32]

More recently, approaches to image CM apoptosis with molecular MRI have been developed.[33] Annexin V was conjugated to the magnetofluorescent nanoparticle, CLIO-Cy5.5, to yield the magnetofluorescent annexin, AnxCLIO-Cy5.5.[33,34] This construct has a level of biological activity similar to that of unmodified annexin, and has been shown to colocalize strongly with Annexin-fluorescein isothiocyanate.[33,34] AnxCLIO-Cy5.5 has been used to image CM

apoptosis by MRI in vivo in a mouse model of ischemia reperfusion (Figure 3).[33] Annexin has also been conjugated to a small gadolinium loaded liposome and used to image CM apoptosis in an isolated perfused heart model.[35] The ability of this construct to be used in vivo, however, will require further study.

The role of apoptosis in plaque rupture is being increasingly appreciated. Apoptosis of plaque macrophages, in particular, has been associated with plaque destabilization and rupture. Moreover, the uptake of technetium-labeled annexin in plaques with high macrophage content has been documented in both animal models and humans (Figure 3).[36,37] Molecular imaging of apoptosis may thus play an important future role in facilitating the development of novel therapies for diseases of both the myocardium and vulnerable atherosclerotic plaque. Techniques to image cellular necrosis are highly complementary and synergistic with those to image apoptosis, and are discussed in more length in the section on ischemia below.

Fibrosis and Scarring

In ischemic heart disease and heart failure, 2 distinct forms of fibrosis are of interest: the fibrosis that characterizes the healed myocardial infarct and the fibrosis that may occur in the remote myocardium not subject to previous ischemic injury. Delayed-enhancement cardiac magnetic resonance has proven highly valuable in detecting both acute and chronic forms of myocardial injury. However, the gadolinium chelates commonly used in delayed-enhancement cardiac magnetic resonance studies are not targeted agents, with the time-dependent enhancement depending on both myocardial blood flow and volume of distribution.[38] Thus when delayed-enhancement cardiac magnetic resonance provides for the direct visualization of necrotic and scarred tissue, conventional contrast agents are unable to distinguish between the 2. Recently, however, a collagen-targeted MRI contrast agent was developed for the molecular imaging of fibrosis[39] that was subsequently used to characterize postinfarction myocardial scarring in a murine model.[40] Figure 4 shows a short-axis CMR image acquired before and after the injection of the collagen-targeted contrast agent (EP-3533), and a corresponding tissue slice in which collagen was stained with Picrosirius red.

Vascular Remodeling

Vascular remodeling is a key pathological attribute in atherosclerosis, aneurysm formation, postangioplasty restenosis, and graft arteriosclerosis. Vascular remodeling involves changes in the vessel diameter or structure. Neointima formation secondary to vascular smooth muscle cell (VSMC) proliferation and migration, extracellular matrix reorganization and concurrent inflammation are important players in the remodeling process.

Targeting VSMC proliferation is a promising approach for early detection of vessel wall hyperplasia. Z2D3, an antibody to a membrane lipid antigen present on proliferating VSMCs, localized to the neointima of injured aorta of high-lipid fed rabbits,[41] and its uptake correlated with VSMC proliferation rate.[42] The feasibility of imaging vascular remodeling in coronary arteries was originally demonstrated by ^{111}In-Z2D3 F(ab′)$_2$ planar imaging in a swine model of intimal proliferation after coronary stenting.[43]

Integrins, a family of heterodimeric cell surface glycoprotein adhesion molecules, mediate cell-extracellular matrix and cell-cell interactions, and are involved in cell adhesion, proliferation, migration, differentiation, and serve as potential targets for imaging of vascular remodeling. The $\alpha v\beta_3$ integrin is expressed by endothelial cells (ECs), VSMCs,[44] platelets, growth factor-stimulated monocytes and T lymphocytes,[45,46] is upregulated early in response to vascular injury, and appears to be a suitable target for imaging of cell proliferation. An ^{111}In-labeled peptidomimetic tracer (RP748, Lantheus) with high affinity for the active conformation of $\alpha v\beta 3$ integrin localized to injured arteries in a model of mechanical injury to carotids of

apoE$^{-/-}$ mice, and closely tracked the proliferative component of vascular remodeling.[47] RP748 was also useful for imaging cell proliferation in a chimeric human/mouse model of graft arteriosclerosis, permitting tracking of the remodeling component of transplant vasculopathy.[48] Gadolinium loaded liposomes, targeted to the $\alpha v\beta 3$ integrin, have been used in a theranostic (diagnostic and therapeutic) approach in a rabbit model of balloon injury and restenosis. The liposomes were loaded with rapamycin, which successfully inhibited restenosis without delaying endothelial repair.[49] MMPs are a large family of endopeptidases that selectively digest matrix and other key proteins, and play an important role in reorganizing vascular matrix scaffold and facilitating cell migration. VSMCs and macrophages are major sources of MMP production. A broad-spectrum radiolabeled MMP inhibitor, [^{123}I]I-HO-CGS 27023A, was used to image MMP presence in ligated carotid arteries in apoE$^{-/-}$ mice.[50] An ^{111}In-labeled small molecule with broad specificity for activated MMPs (RP782, Lantheus) has been used for in vivo microSPECT/CT imaging of the remodeling process following mechanical injury in apoE$^{-/-}$ mice.[51]

Angiogenesis

Angiogenesis is a complex process, which involves (1) degradation of the basal membrane surrounding the parental vasculature, (2) migration of ECs or progenitor cells, (3) proliferation of quiescent ECs to form new vessels, and (4) alignment and organization of ECs to form tubes.[52,53] The process of angiogenesis involves the interplay of many cells including monocytes/macrophages, mast cells, lymphocytes, connective tissue cells, pericytes, ECs and pluripotent progenitor cells, all of which influence the process by secreting soluble angiogenic and antiangiogenic molecules including extracellular matrix and proteolytic enzymes. Targeted imaging of biological markers will be critical for understanding the angiogenic process and tracking novel molecular or genetic therapies. Potential targets for imaging of angiogenesis fall into 3 principal categories; (1) EC markers of angiogenesis; (2) non-ECs involved with angiogenesis; and (3) markers of the extracellular matrix.

Perhaps the most widely used strategy for molecular imaging of either adaptive or pathological angiogenesis has been to target endothelial integrins that participate in vasculogenesis or remodeling. For the most part, probes have been targeted to specific matrix-binding integrin heterodimers that signal EC migration, proliferation and survival such as a_v-integrins ($\alpha_v\beta_3$, $\alpha_v\beta_5$) and a_5-integrins.[54,55] Specificity for angiogenic vessels is somewhat decreased when diffusible rather than pure intravascular imaging probes are used because inflammatory cells and fibroblasts can express many of these integrins. Nonetheless, imaging of $\alpha_v\beta_3$ with targeted radionuclide and PET probes have been shown to detect angiogenesis in recent myocardial infarction in animals and in humans (Figure 5).[56,57] These tracers tend to localize in regions where perfusion is most profoundly reduced.[56] In models of chronic limb ischemia without necrosis, targeted $\alpha_v\beta_3$ radiotracer-based imaging[58] or targeted contrast ultrasound of only endothelial α_v-integrin expression has been shown to detect both endogenous and growth-factor stimulated arteriogenesis, and to predict future flow recovery.[59] Because neovascularization in atherosclerotic lesions is also characterized by α_v-integrin expression, the strategy of targeting $\alpha_v\beta_3$ with MRI probes has been used to detect atherosclerotic disease in animal models.[60]

Targeted imaging of growth factor receptors has also been used to detect vascular remodeling. Growth factor imaging has most frequently relied on either using radionuclide-labeled vascular endothelial growth factor (VEGF) isoforms as a targeting moiety, or antibodies against specific VEGF signaling receptors such as flk-1 (KDR).[61,62]

The immune response plays a critical role in angiogenesis and arteriogenesis, in part by providing a source for proangiogenic growth factors (VEGFs, fibroblast growth factors, platelet-derived growth factor), cytokines (interleukin-1, tumor necrosis factor-α, CCL2,

CD40L), and proteases required for vascular sprouting and/or remodeling. Gene-targeted deletion of adhesion molecules or cytokine receptors that mediate the inflammatory response results in impaired arteriogenesis in ischemic tissues.[63,64] Targeting contrast ultrasound imaging of monocyte recruitment and EC adhesion molecule (vascular cell adhesion molecule-1 [VCAM-1]) expression has recently been shown to herald vascular remodeling in limb ischemia before any significant flow recovery (Figure 5).[65] This strategy also has been used to detect immune response dysfunction associated with impaired arteriogenesis.[65] In a related matter, immune cell activity is probably reflected by the signal from diffusible imaging probes targeted to matrix proteases that participate in tissue and vascular remodeling. These probes have been shown to enhance in recent MI and in proliferative atherosclerotic lesions and reflect key regulatory processes in neovessel formation or development of collaterals.[66,67]

Targeting Specific Cardiovascular Diseases

Atherosclerosis

Atherosclerosis is characterized by the thickening of the arterial wall to form an atherosclerotic plaque, a process in which cholesterol deposition, inflammation, extracellular-matrix formation and thrombosis have important roles.[4,68] Symptoms occur late in the course of disease and are usually caused by the narrowing of the lumen of the artery, which can happen gradually (as a result of progressive plaque growth) or suddenly (as a result of plaque rupture and, subsequently, thrombosis). The resultant decrease in blood supply can affect almost any organ, although coronary heart disease and stroke are the most common consequences.

Traditionally, diagnosis of atherosclerosis was possible only at advanced stages of disease, either by directly revealing the narrowing of the arterial lumen (stenosis) or by evaluating the effect of arterial stenosis on organ perfusion. However, new imaging approaches allow the assessment not only of the morphology of blood vessels but also of the composition of the vessel walls, enabling atherosclerosis-associated abnormalities in the arteries (including the coronary arteries) to be observed, down to the cellular and molecular level.

Because inflammation has a crucial role at all stages of atherosclerosis, macrophages are currently one of the most appealing targets. Ultrasmall long-circulating superparamagnetic iron-oxide nanoparticles are engulfed by macrophages in vivo, and this causes a detectable decrease in the MRI signal in proportion to the degree of atherosclerotic plaque inflammation, as shown in human studies.[69] These nanoparticles can also be derivatized with optical and nuclear reporters to facilitate validation with fluorescence techniques and use of PET to enhance sensitivity.[70] A strong correlation between macrophage density and MRI signal was also found recently in a mouse model of atherosclerosis, by using a contrast agent consisting of Gd3+-loaded micelles targeted to the macrophage scavenger receptor.[71] This same technique has also been used to image oxidized low-density lipoprotein in atheromatous plaques with MRI (Figure 6).[72] Using bio-mimicry and lipoproteins, such as high-density lipoprotein, a multimodal molecular imaging probe for macrophages has been demonstrated to be very flexible.[73,74] Similarly, in rabbits, specific uptake of an iodine-containing contrast agent by macrophages allows inflamed atherosclerotic lesions to be detected with CT (Figure 6).[75] The signal from [18F]fluorodeoxyglucose correlates with the concentration of macrophages in human atherosclerotic plaques.[76] The concurrent use of several imaging techniques—for example, PET together with CT or, recently, MRI[77]—enables sensitive and reproducible detection of vascular inflammation.[78,79] This hybrid approach allows the most appropriate technique for a particular patient, vascular region, and disease stage to be chosen and takes advantage of the particular strengths of each modality.

The early detection of disease is one of the principal aims of molecular imaging. Cell-adhesion molecules participate in the early development of atherosclerotic lesions by facilitating the recruitment of leukocytes into the vessel wall. Increased amounts of vascular cell-adhesion molecule 1 (VCAM-1) were found in aortic plaques of apoE$^{-/-}$ mice by using a dual contrast agent detectable by both MRI and fluorescence imaging (Figure 6).[80] Another possibility is to use probes that emit a detectable signal only after they have been activated by the target. For example, in a recent study in rabbits, a fluorescent probe activated by enzymatic degradation was used to reveal intraplaque protease activity with a near-infrared fluorescence intravascular catheter.[81] In addition, nuclear reporters, capable of detecting the presence of proteases, have been synthesized (Figure 6).[50,51]

Targeted probes can also be used for therapeutic purposes to deliver drugs in a targeted manner. The potential of this strategy was demonstrated in a study in which rabbits were administered paramagnetic nanoparticles loaded with an antiangiogenic drug. The subsequent reduction in the extent of new blood vessel formation in the atherosclerotic plaques could be monitored noninvasively with MRI by imaging the extent of nanoparticle uptake.[82]

Ischemic Injury

Myocardial damage during ischemic injury is mediated by the following 3 distinct processes: (1) the ischemic episode itself, (2) reperfusion following the ischemic episode, and (3) the inflammatory response to the ischemic event. CM death during ischemic injury can be mediated through either apoptosis or necrosis. Apoptotic cell death dominates during the first 4 to 6 hours of injury,[83] after which necrosis becomes the dominant form of cell death. Molecular imaging of CM apoptosis is discussed extensively above. A necrosis specific imaging agent (based on an antimyosin antibody) has been developed for both nuclear and MR application.[84,85] Myosin is an intracellular protein that cannot be accessed by an antibody when the cell membrane is intact. Rupture of the cell membrane during CM necrosis, however, allows the antimyosin antibody to access and bind to its target. Radiolabeled antimyosin antibodies have been used to image CM necrosis in vivo in animal models and in patients with a broad range of conditions including acute coronary syndromes and myocarditis.[84,86] An MR-detectable antimyosin agent has also been described,[85] however, the experience with this agent is considerably less extensive.

Acute ischemia leads to the expression of adhesion molecules on the ischemic endothelium. These adhesion molecules play an important role in mediating the subsequent migration of neutrophils into the injured myocardium. Ultrasound microbubbles labeled with ligands to selectins have been shown to detect the expression of adhesion molecules in ischemic myocardium.[87,88] An antibody to P-selectin has also been conjugated to micron-sized iron oxide nanoparticles,[17] and VCAM-1 expression has been imaged with a targeted magnetofluorescent nanoparticle.[80] Several platforms, thus, exist to image the endothelial expression of adhesion molecules in active and recently ischemic myocardium.

Neutrophil migration into ischemic myocardium begins within a few hours of the ischemic event and peaks within the first 24 hours of injury. This is followed by biphasic monocyte recruitment, with an inflammatory monocyte subset dominating on the first 2 to 3 days and a second subset that promotes angiogenesis dominant on days 4 to 7.[10] A molecular contrast agent, targeted to the leukotriene B4 receptor, and capable of selectively imaging neutrophil infiltration of the myocardium, has previously been described.[89] In addition, the imaging of monocyte/macrophage infiltration into ischemic myocardium can be robustly imaged with both MRI and fluorescence tomography.[6,90] Long circulating iron oxide nanoparticles are avidly taken up by macrophages infiltrating the myocardium, which can then be imaged in vivo with both T2*-weighted (negative contrast),[90] and off resonance (positive contrast) MRI,[91] (Figure 7). A highly linear relationship was seen between the dose of nanoparticles injected and the

amount of contrast generated in the myocardium.[90] Labeling the nanoparticles with a near infrared fluorochrome also allowed the infiltrating monocytes/macrophages to be imaged in vivo with fluorescence tomography.[90]

Postinfarction Remodeling

During the first 2 weeks after MI, innate immunity mounts an inflammatory response in the infarcted tissue that evolves into a complex wound healing process. Poor healing can result in infarct expansion and adverse remodeling of remote areas of the myocardium, resulting in chamber dilation and hypertrophy, and a downward spiral leading to overt heart failure.[92] Targeted imaging of components of the inflammatory and healing processes can predict remodeling in animal models. During the early inflammatory phase, the extent and quality of neutrophil and monocyte subset influx regulates subsequent stages of infarct healing.[10] These innate immune cells have been imaged in murine models with activatable gadolinium-serotonin chelates[93] and nanoparticles that can be detected optically or with MRI.[6,90] Furthermore, key enzymes that are released by monocyte/macrophages can be targeted with optical,[6] MRI[93] and nuclear reporters.[67] Specifically, MMPs and cathepsins degrade the preexisting, necrotic extracellular matrix within the infarct area and can be imaged quantitatively with activatable "smart" agents.[6,8] The presence of MMP in the infarct has been quantified by nuclear imaging in several animal models by targeting the active site of this enzyme with small molecules tagged with SPECT isotopes.[67] Both, the presence of macrophages[10] and the activity of released proteases have been related to prognosis in animal models,[94] which may open a diagnostic and consequently a therapeutic window to augment healing processes. In later stages of wound healing, integrins have been imaged to follow angiogenesis, which is crucial for the supply of evolving granulation tissue.[56] Furthermore, the transglutaminase Factor XIII has been shown to play an important role in organizing the new matrix in the scar[95] with clinically relevant sequelae.[96] FXIII has been imaged with an ^{111}In-labeled peptide substrate that becomes crosslinked to surrounding matrix proteins in the evolving scar (Figure 7).[97] These studies have shown that imaging tools that follow inflammation and healing after MI can successfully identify individuals at risk of heart failure, and may in future be used to personalize therapy.

Heart Failure

It is well established that local activation of the reninangiotensin system contributes to heart failure, and thus a number of targeted agents have been developed to probe the function of the reninangiotensin system by molecular imaging methods.[98] One approach involves radiolabeling ACE inhibitors for detection by SPECT or PET, whereas another focuses on the angiotensin II type 1 receptor (AT1) by radiolabeling AT1 receptor antagonists.[98] Recent data suggest that heart failure can be characterized in terms of an innate immune response to diverse forms of tissue injury.[99] Because NF-κB plays a central role in proinflammatory responses, a noninvasive assessment of NF-κB expression might offer new insight into the role of inflammatory activation during heart failure. Toward this end, a transgenic mouse expressing luciferase under the control of the NF-κB promoter was used to noninvasively characterize NF-κB expression over time after myocardial infarction using bioluminescence imaging (BLI).[100] In the setting of ischemic heart failure, viable myocardium often exhibits a shift in substrate utilization from aerobic (free-fatty acids) to anaerobic (glucose) metabolism. PET and SPECT probes for assessing myocardial metabolism were summarized in Part I of this Series, including 2-(^{18}F) fluoro-2-deoxy-D-glucose (FDG) for assessing glucose uptake by PET and ^{123}I-β methyl-P-iodophenylpentadecanoic acid for assessing free fatty acid uptake by SPECT. Heart failure is also characterized by dysfunctional baroreceptor reflex control and elevated levels of plasma norepinephrine. Elevated plasma norepinephrine is a strong predictor of mortality in patients with advance heart failure,[101] and is associated with the downregulation and uncoupling of β-adrenergic receptors in cardiac myocytes. Part I of this series reviewed a radiolabeled β-blocker for PET imaging (^{11}C-CGP12177) with potential utility in assessing

β-adrenergic receptor function in the setting of heart failure.[1] Part I also reviewed approaches for measuring presynaptic function by PET using ^{11}C-meta-hydroxyephedrine or by SPECT using ^{123}I-meta-iodobenzylguanidine.[1] Apoptosis and an imbalance of the myocardial flow/function and angiogenesis/hypertrophy relationship plays a major role in the pathogenesis of heart failure. Thus, targeted imaging of apoptosis and angiogenesis (described earlier) might also prove diagnostic in certain forms of heart failure.

Transplant Rejection

The current clinical standard for graft surveillance consists of serial endomyocardial biopsies. However, this procedure suffers from a substantial sampling error and complications. These limitations and the discomfort of the invasive procedure motivated assessment of molecular imaging techniques to report on organ rejection. One of the first attempts to image heart transplant rejection used an ^{111}In-labeled antibody targeted to myosin, the intracellular contractile protein that is shielded behind the cell membrane in intact myocytes.[102] ^{99m}Tc-labeled annexin-V has been used to image rejection in patients after heart transplantation.[32] Ho and colleagues harnessed the high propensity of dextrancoated iron oxide nanoparticles for uptake by phagocytes to image rejection by MRI. They used long circulating macrophage-avid iron oxide nanoparticles in rats with transplant rejection, and found a 30% signal change 24 hours after injection[103] and a good correlation between signal change in MRI and pathological rejection grade. The same group used micron-sized iron oxide particles to image macrophage uptake in rejected cardiac grafts in rats,[104] with a more punctuate change in MR signal. BLI has been used to monitor graft survival in rodents.[105] Although this work introduces an elegant research tool to monitor graft survival noninvasively, clinical translation of BLI is not feasible. Using an ultrasound-based approach, Weller et al[106] designed microbubbles that target the adhesion molecule ICAM-1, which allowed detection of graft rejection of heterotopic heart transplants in rats.

Monitoring Cell-Based Therapies

Iron oxide nanoparticles yield negative contrast on T2*-weighted images even with small intracellular amounts and appear to have a wide safety profile with little effect on cellular function.[107,108] Transfection agents or electroporation are used to encourage cellular uptake in nonphagocytic cells.[109,110] Using delayed contrast enhanced MRI for guidance during interventional MRI, targeting of the injections to the peri-infarcted region of the myocardium can be performed.[111,112] Because the majority of the adult stem cells does not survive and engraft, there remains an intense debate as to whether hypointensities imaged at later time points represent intact, live engrafted cells, residual free iron, or iron within macrophages.[113,114] Direct labeling of cells with fluorinated compounds[115] has also been used and suffers from similar limitations as iron oxide labeling. Rapid cell proliferation and division may dilute the label in the daughter cell—leading to the inability to detect labeled cells after 6 to 8 cell divisions.[116] Even without cell division, the reliable detection limit of a cluster of iron oxide-labeled cells in the beating heart at clinical field strengths is on the order of 100 000 cells.[117] Therefore, detection of iron oxide-labeled stem cells after intravenous injection is difficult due to the small number of cells that home to injured myocardium.[118] The strength of direct cell labeling with iron oxide nanoparticles is the ability to determine the initial delivery of the cellular therapeutic to the heart without exposing the stem cells or the patient to ionizing radiation. A new novel method to enhance stem cell viability and enable cell tracking has been the addition of MRI-labeled cells to tissue matrices[119] or the addition of contrast agents to microencapsulation materials.[120] In the latter case, the imaging label can be added at a higher concentration to the porous barrier than would be possible for intracellular labeling without compromising cell viability. Indeed, radiopaque contrast agents have now been used to create x-ray–visible stem cells. This new technique may provide the ideal marriage of stem cell

labeling with current cardiovascular interventional techniques that are primarily x-ray based (Figure 8).

Reporter gene imaging of stem cells overcomes some of the limitations of direct cell labeling. Here, the stem cells are genetically modified to express reporter genes before transplantation. The reporter gene DNA construct can be transferred into cells via a viral (eg, lentivirus, retrovirus, adenovirus, adeno-associated virus) or nonviral vector (eg, plasmid). Translation of the reporter gene mRNA produces a protein, that when exposed to the complementary probe, generates an imaging signal.[121] Commonly used promoters are constitutive (continuous expression), inducible (controlled expression), or cell/tissue specific. Varying the promoter sequence can provide information about stem cell differentiation and mechanism of therapy. For example, including a cardiac specific promoter (eg, α-cardiac myosin heavy-chain promoter) that will express a reporter gene when the cells differentiate into cardiac phenotype will allow selection of cardiac differentiated cells among undifferentiated stem cells.

Frequently used reporter gene imaging constructs include firefly luciferase (*Fluc*)-based optical bioluminescence (BLI),[122,123] sodium-iodide symporter (*NIS*) for SPECT imaging,[124] and herpes simplex virus thymidine kinase (*HSV-tk*)-based PET imaging.[125,126] For BLI, the reporter gene is *Fluc*, which oxidizes the substrate D-Luciferin to produce light, similar to how light is generated within the firefly insect (Figure 8). However, this technique is restricted to small animal use because the emitted photons become attenuated within deep tissues and thus are currently not applicable to large animal or human studies. By contrast, the *HSV-tk* reporter gene constructs have been applied to large animals[126–128] and in human studies involving adoptive cell transfer.[129] The basis behind this approach is injecting the subject with a radiolabeled thymidine analogue (eg, [18F]fluoro-3-hydroxymethylbutylguanine or [^{18}F]-FHBG) that can be detected by PET when it is phosphorylated by *HSV-tk* and subsequently trapped inside the cell. A drawback to *Fluc, NIS,* and *HSV-tk* is that the stem cells must be genetically modified before transplantation. However, the advantage is that only viable cells will produce a signal. Likewise, proliferation of stem cells stably expressing the reporter gene can be detected by progressive rise of imaging signals over time. Finally, if the transplanted cells are apoptotic or dead, the reporter genes will be absent, thus minimizing false signals.

Because each imaging modality possesses unique limitations and advantages, multimodality imaging constructs have been developed that combine the best features of each technology in an attempt to satisfy all the needs of stem cell imaging. One example is the triple fusion reporter gene construct that consists of monomeric red fluorescence protein (*mRFP*), *Fluc*, and *HSV-tk.*[125,126] Each portion of the multimodality imaging construct provides its unique benefits: *mRFP* allows isolation of the stably transduced cell population and *Fluc* enables high throughput in small animal models. In addition, *HSV-tk* enables PET imaging in small animals, large animals, and patients.

Monitoring Gene Therapy

Gene therapy aims at the vector-mediated overexpression of endogenous or exogenous genes for molecular intervention with the disease process. It has been tested in various cardiovascular diseases, including ischemia, heart failure and arrhythmias. Many basic tools and principles remain under development, and questions concerning delivery methods, therapeutic efficacy and safety remain open. Molecular imaging provides valuable tools to address these open issues noninvasively.[130]

To track the therapeutic agent directly, the advent of cardiac gene therapy has promoted the development of reporter gene imaging techniques for the heart. Following gene transfer, detection of the level of reporter gene product activity is achieved through accumulation of a reporter probe which provides indirect information on the level of reporter gene expression,

but also reflects endogenous signaling and transcription factors which drive reporter gene expression. The gene product of suitable reporter genes is usually not present in target tissue and has little effects or interaction with tissue function. It can be an enzyme that catalyzes specific accumulation of an imaging reporter probe (eg, HSV-tk accumulating radiolabeled nucleosides, luciferase metabolizing luciferin for light production),[127,131,132] a receptor which accumulates specific receptor ligand probe (eg, dopamine D2 receptor accumulating radiolabeled ligands),[133] or a transport protein which results in intracellular accumulation of specific probe molecules (eg, NIS accumulating radioiodine, iron nanoparticles, or technetium).[134] This technique has been initially introduced using autoradiography,[135] and has since been translated from small rodents[136] to large experimental animals,[127,128] where it allows for noninvasive assessment of location, magnitude and persistence of transgene expression. Coexpression of a reporter gene will allow for indirect imaging of the expression of a therapeutic gene of choice,[137,138] and linkage of measures of transgene expression to downstream functional effects will enhance the understanding of basic mechanisms of cardiac gene therapy (Figure 8).[139] More recently, it has also been suggested that reporter gene imaging can be used for imaging of more specific myocardial conditional gene activation.[140]

Integrative and Multimodal Approaches

A successful molecular imaging strategy requires the use of a sensitive and specific agent to the target of choice, the ability to image the anatomic distribution of the agent with a high degree of certainty and spatial resolution, and the ability to integrate the molecular and anatomic images with a functional or physiological readout in that organ. The breadth and flexibility of molecular MRI allows these requirements to be met in many scenarios.[2] However, molecular MRI has significantly lower sensitivity than SPECT, PET and fluorescence techniques.[3] SPECT, PET and fluorescence on the other hand do not provide adequate anatomic information and have significantly lower resolution. A compelling case can thus be made for a multimodal imaging approach that exploits the strengths of several modalities.

At the preclinical level, high resolution small animal PET-CT and SPECT-CT systems are becoming increasingly standard. However, cardiovascular structures in mice are often of submillimeter in diameter, which profoundly challenges the spatial resolution of nuclear and fluorescence imaging. Prototypes of integrated FMT-CT and FMT-MR systems are therefore under development. Integration of CT and MRI with PET and FMT datasets has been performed offline by including fiducial markers in the field of view, and by using advanced shape/pattern recognition software that supports off-line fusion at submillimeter precision. Unlike PET-CT systems, where the images are acquired sequentially, MR-PET systems have been designed to perform the acquisition of the MR and PET signals simultaneously.[141] Whole body MR-PET systems for human imaging are currently under development and will likely play an important role in cardiovascular imaging.

The concept of hybrid imaging can be extended even further by performing multimodal molecular imaging with several platforms. This could allow a cluster of biomarkers to be imaged together in a systems approach. The combination of fluorescence, MRI and PET or SPECT imaging, for instance, could allow >4 targets to be imaged at one time. Potential applications of this strategy include inflammatory atherosclerosis where imaging of the adhesion molecule VCAM-1 could be performed with a PET reporter, the recruitment of monocyte/macrophages could be imaged with magnetofluorescent nanoparticles, and the assessment of their proteolytic activity could be detected with near infrared protease sensors. This comprehensive molecular imaging strategy would offer a global view of events, rather than focusing in isolation on a single molecule.

Potential Clinical Impact

Molecular imaging has the potential to impact cardiovascular medicine in several ways, including the assessment of risk, the early detection of disease, the development of personalized and targeted therapeutic regimens, and the monitoring of therapeutic efficacy and outcome. In addition to these direct implications, molecular imaging will affect clinical care indirectly by facilitating the more rapid development of novel pharmaceuticals and improving the basic understanding of cardiovascular pathophysiology.

The clinical role of cardiovascular molecular imaging is still emerging, although several completed studies involving clinical patients have already demonstrated the feasibility and potential value of molecular imaging. The established clinical value of metabolic imaging and neuroreceptor imaging was previously outlined in Part I of this consensus.[1] Other examples of targeted clinical imaging include the uptake of ^{99m}Tc-labeled annexin-V[36], iron oxide nanoparticles[142] or ^{18}F-deoxyglucose in carotid plaques in humans, which has been associated with macrophage rich plaques and clinical instability.[76,78,143] These agents could thus conceivably be used to detect plaque vulnerability in appropriately selected patient populations. The fibrin sensing gadolinium chelate EP2104R has now been given to patients with a clinical suspicion of thrombosis, and could play a valuable role in the diagnosis and monitoring of deep venous thrombosis, pulmonary embolism, left atrial appendage thrombosis and embolic stroke.[21] The uptake of ^{99m}Tc-annexin-V has also been shown to predict an adverse clinical course in patients with heart failure, and also potential rejection in patients with heart transplantation.[31,32]

As the cost and complexity of clinical care continue to escalate, an algorithmic approach to patient therapy based on outcome results from large clinical trials will need to be complemented by a personalized approach involving biomarkers and molecular imaging. The initial clinical experience with gene or stem cell therapy for treatment of ischemic heart disease, for instance, has been inconsistent and difficult to interpret in the absence of molecular imaging specifically targeted at the biological end point (ie, angiogenesis or myocardial repair). The simple evaluation of clinical outcomes or physiological consequences may be too insensitive to detect a potential true biological effect. Therefore, complex new therapies of this sort will require molecular imaging for a more sensitive and robust assessment of their therapeutic efficacy.

Barriers to Translation

The attributes and limitations of each of the imaging modalities reviewed in Part I of this consensus document present a unique set of translational challenges specific to each modality. SPECT and PET imaging offer high sensitivity, relatively low cost, and a minimal potential for adverse bioeffects, providing the quickest route for translation of molecular imaging to patients. However, this advantage needs to be balanced by the additive exposure to ionizing radiation associated with serial nuclear imaging. The importance of this radiation exposure in cardiovascular imaging is being increasingly realized and is of particular relevance to molecular imaging, which could involve serial imaging of otherwise young healthy people. In addition, the limited resolution of nuclear imaging requires anatomic colocalization of nuclear images with higher resolution anatomic x-ray CT images particularly if absolute quantification of the targeted radiotracers is required. Although the use of hybrid SPECT-CT and PET-CT imaging systems will clearly improve the accuracy of nuclear-based molecular imaging approaches, the benefit of this additional quantitative accuracy will come at the cost of exposure to 2 sources of ionizing radiation. Although many clinical scenarios will arise where the risks of radiation exposure will be far out weighted by the information obtained from the hybrid nuclear-CT molecular images, this will need to be carefully assessed on a case-by-case basis.

The lower sensitivity of MR-based molecular imaging approaches creates the principal barrier to their clinical translation. Highly expressed targets, such as fibrin and type 1 collagen, can be imaged with small gadolinium chelates that have pharmacokinetics very similar to those of clinically used gadolinium chelates. However, many other targets in the cardiovascular system are focal or of low volume and require agents with much higher sensitivity. Gadolinium containing nanoparticles provide the required increase in sensitivity but their pharmacokinetics and elimination are complex. The potential for tissue retention of gadolinium and subsequent systemic fibrosis will need to be rigorously addressed with all gadolinium-based probes, but will be of particular importance in the case of activatable and nanoparticulate gadolinium-containing constructs.

The clinical experience with iron-oxide nanoparticles for liver and lymph node imaging is fairly extensive and has revealed an excellent safety profile.[144] However, the safety of these agents for serial imaging studies will need to be more rigorously addressed. Clear dosing guidelines will need to be developed to avoid any risk of iron overload. The risk of an immune reaction to the material coating the nanoparticle associated with repeat injections will also need to be carefully assessed. The advantages of MR-based molecular imaging, which does not involve exposure to ionizing radiation, will need to be weighed carefully against the more complex pharmacokinetics of these agents.

Fluorescence molecular tomography (FMT) is an extremely valuable technique for molecular imaging of small animal that cannot be easily translated to humans with current detector technology. However, noninvasive fluorescence imaging of large superficial vessels such as the carotid and femoral arteries might be possible. In contrast, fluorescence imaging of the coronary arteries will undoubtedly require the use of intravascular optical catheters, a prototype of which has recently been developed.[81] Organic NIR cyanine fluorochromes, such as indocyanine green, have been used clinically for many years and are highly analogous to experimental NIR fluorochromes that are currently entering phase 1 clinical trials. The use of quantum dots for fluorescence imaging in clinical practice, however, remains unlikely due to the highly toxic moieties contained within these agents.

The routine application of molecular imaging in the management of patients with cardiovascular disease is likely close. Molecular imaging should develop further with appropriate education of the cardiovascular community and the increased availability of various hybrid imaging systems (SPECT-CT, PET-CT, PET-MRI) that will facilitate quantification of molecular imaging agents. A number of challenges, however, stand in the way of realizing these promises. Current imaging systems have not been optimized for cardiac applications, with inadequate correction for cardiac and respiratory motion and a lack of quantitative software for targeted agents. Full realization of the promise of cardiovascular molecular imaging will thus require an ongoing and concerted collaboration between industry, and the basic science and imaging communities.

Conclusion

As the field of molecular imaging gains momentum, we will see a continuously increasing number of imaging biomarkers in preclinical and clinical studies. Preclinical research will continue to be accelerated by noninvasive, sensitive, and longitudinal assessment of therapeutic targets. “Smart” amplification strategies, comparative head-to-head analysis of markers, improved reporter performance, and improving hardware will enable us to detect minuscule or trace amounts of novel targets. These noninvasive targeted approaches will have to be tested for their prognostic value, cost effectiveness, and potential long term toxicity to translate these technological advances into improved patient care.

Acknowledgments

Sources of Funding

This work was supported in part by American Heart Association Scientist Development Grant 0835623D (to M.N.); National Institutes of Health grants R01 HL093038 and K08 HL079984 (to D.E.S.); grant R01 HL085093 and a Department of Veterans Affairs Merit Award (to M.M.S.); grant R21/R33 HL089027 (to J.C.W.); grants R21/R33 HL089029, 2008-MSCRFII-0399-00 (Maryland Stem Cell Research Fund), and R01 EB007825 (to D.L.K.); and grants R01 HL078650 and R01 HL065662 (to A.J.S.).

References

1. Sinusas AJ, Bengel FM, Nahrendorf M, Epstein FH, Wu JC, Villanueva FS, Fayad ZA, Gropler RJ. Multimodality Cardiovascular Molecular Imaging, Part 1. Circ Cardiovasc Imaging 2008;1:244–256. [PubMed: 19808549]
2. Sosnovik DE, Nahrendorf M, Weissleder R. Molecular magnetic resonance imaging in cardiovascular medicine. Circulation 2007;115:2076–2086. [PubMed: 17438163]
3. Wu JC, Bengel FM, Gambhir SS. Cardiovascular molecular imaging. Radiology 2007;244:337–355. [PubMed: 17592037]
4. Sanz J, Fayad ZA. Imaging of atherosclerotic cardiovascular disease. Nature 2008;451:953–957. [PubMed: 18288186]
5. Weissleder R, Pittet MJ. Imaging in the era of molecular oncology. Nature 2008;452:580–589. [PubMed: 18385732]
6. Nahrendorf M, Sosnovik DE, Waterman P, Swirski FK, Pande AN, Aikawa E, Figueiredo JL, Pittet MJ, Weissleder R. Dual channel optical tomographic imaging of leukocyte recruitment and protease activity in the healing myocardial infarct. Circ Res 2007;100:1218–1225. [PubMed: 17379832]
7. Chen J, Tung CH, Mahmood U, Ntziachristos V, Gyurko R, Fishman MC, Huang PL, Weissleder R. In vivo imaging of proteolytic activity in atherosclerosis. Circulation 2002;105:2766–2771. [PubMed: 12057992]
8. Chen J, Tung CH, Allport JR, Chen S, Weissleder R, Huang PL. Near-infrared fluorescent imaging of matrix metalloproteinase activity after myocardial infarction. Circulation 2005;111:1800–1805. [PubMed: 15809374]
9. Kircher MF, Grimm J, Swirski FK, Libby P, Gerszten RE, Allport JR, Weissleder R. Noninvasive in vivo imaging of monocyte trafficking to atherosclerotic lesions. Circulation 2008;117:388–395. [PubMed: 18172031]
10. Nahrendorf M, Swirski FK, Aikawa E, Stangenberg L, Wurdinger T, Figueiredo JL, Libby P, Weissleder R, Pittet MJ. The healing myocardium sequentially mobilizes two monocyte subsets with divergent and complementary functions. J Exp Med 2007;204:3037–3047. [PubMed: 18025128]
11. Swirski FK, Pittet MJ, Kircher MF, Aikawa E, Jaffer FA, Libby P, Weissleder R. Monocyte accumulation in mouse atherogenesis is progressive and proportional to extent of disease. Proc Natl Acad Sci USA 2006;103:10340–10345. [PubMed: 16801531]
12. Swirski FK, Berger CR, Figueiredo JL, Mempel TR, von Andrian UH, Pittet MJ, Weissleder R. A near-infrared cell tracker reagent for multiscopic in vivo imaging and quantification of leukocyte immune responses. PLoS ONE 2007;2:e1075. [PubMed: 17957257]
13. Auffray C, Fogg D, Garfa M, Elain G, Join-Lambert O, Kayal S, Sarnacki S, Cumano A, Lauvau G, Geissmann F. Monitoring of blood vessels and tissues by a population of monocytes with patrolling behavior. Science 2007;317:666–670. [PubMed: 17673663]
14. Bates SM, Lister-James J, Julian JA, Taillefer R, Moyer BR, Ginsberg JS. Imaging characteristics of a novel technetium Tc 99m-labeled platelet glycoprotein IIb/IIIa receptor antagonist in patients With acute deep vein thrombosis or a history of deep vein thrombosis. Arch Intern Med 2003;163:452–456. [PubMed: 12588204]
15. Botnar RM, Perez AS, Witte S, Wiethoff AJ, Laredo J, Hamilton J, Quist W, Parsons EC Jr, Vaidya A, Kolodziej A, Barrett JA, Graham PB, Weisskoff RM, Manning WJ, Johnstone MT. In vivo molecular imaging of acute and subacute thrombosis using a fibrin-binding magnetic resonance imaging contrast agent. Circulation 2004;109:2023–2029. [PubMed: 15066940]

16. Jaffer FA, Tung CH, Wykrzykowska JJ, Ho NH, Houng AK, Reed GL, Weissleder R. Molecular imaging of factor XIIIa activity in thrombosis using a novel, near-infrared fluorescent contrast agent that covalently links to thrombi. Circulation 2004;110:170–176. [PubMed: 15210587]

17. McAteer MA, Schneider JE, Ali ZA, Warrick N, Bursill CA, von zur Muhlen C, Greaves DR, Neubauer S, Channon KM, Choudhury RP. Magnetic resonance imaging of endothelial adhesion molecules in mouse atherosclerosis using dual-targeted microparticles of iron oxide. Arterioscler Thromb Vasc Biol 2008;28:77–83. [PubMed: 17962629]

18. Nair SA, Kolodziej AF, Bhole G, Greenfield MT, McMurry TJ, Caravan P. Monovalent and bivalent fibrin-specific MRI contrast agents for detection of thrombus. Angew Chem Int Ed Engl 2008;47:4918–4921. [PubMed: 18496805]

19. Spuentrup E, Buecker A, Katoh M, Wiethoff AJ, Parsons EC Jr, Botnar RM, Weisskoff RM, Graham PB, Manning WJ, Gunther RW. Molecular magnetic resonance imaging of coronary thrombosis and pulmonary emboli with a novel fibrin-targeted contrast agent. Circulation 2005;111:1377–1382. [PubMed: 15738354]

20. Sirol M, Fuster V, Badimon JJ, Fallon JT, Moreno PR, Toussaint JF, Fayad ZA. Chronic thrombus detection with in vivo magnetic resonance imaging and a fibrin-targeted contrast agent. Circulation 2005;112:1594–1600. [PubMed: 16145001]

21. Spuentrup E, Botnar RM, Wiethoff AJ, Ibrahim T, Kelle S, Katoh M, Ozgun M, Nagel E, Vymazal J, Graham PB, Gunther RW, Maintz D. MR imaging of thrombi using EP-2104R, a fibrin-specific contrast agent: initial results in patients. Eur Radiol 2008;18:1995–2005. [PubMed: 18425519]

22. Fliss H, Gattinger D. Apoptosis in ischemic and reperfused rat myocardium. Circ Res 1996;79:949–956. [PubMed: 8888687]

23. Foo RS, Mani K, Kitsis RN. Death begets failure in the heart. J Clin Invest 2005;115:565–571. [PubMed: 15765138]

24. Yaoita H, Ogawa K, Maehara K, Maruyama Y. Attenuation of ischemia/reperfusion injury in rats by a caspase inhibitor. Circulation 1998;97:276–281. [PubMed: 9462530]

25. Dumont EA, Reutelingsperger CP, Smits JF, Daemen MJ, Doevendans PA, Wellens HJ, Hofstra L. Real-time imaging of apoptotic cell-membrane changes at the single-cell level in the beating murine heart. Nat Med 2001;7:1352–1355. [PubMed: 11726977]

26. Hayakawa Y, Chandra M, Miao W, Shirani J, Brown JH, Dorn GW II, Armstrong RC, Kitsis RN. Inhibition of cardiac myocyte apoptosis improves cardiac function and abolishes mortality in the peripartum cardiomyopathy of Galpha(q) transgenic mice. Circulation 2003;108:3036–3041. [PubMed: 14638549]

27. Faust A, Wagner S, Law MP, Hermann S, Schnockel U, Keul P, Schober O, Schafers M, Levkau B, Kopka K. The nonpeptidyl caspase binding radioligand (S)-1-(4-(2-[18F]Fluoroethoxy)-benzyl)-5-[1-(2-methoxymethylpyrrolidinyl)sulfonyl]isatin ([18F]CbR) as potential positron emission tomography-compatible apoptosis imaging agent. Q J Nucl Med Mol Imaging 2007;51:67–73. [PubMed: 17372575]

28. Korngold EC, Jaffer FA, Weissleder R, Sosnovik DE. Noninvasive imaging of apoptosis in cardiovascular disease. Heart Fail Rev 2008;13:163–173. [PubMed: 18074226]

29. Liu Z, Zhao M, Zhu X, Furenlid LR, Chen YC, Barrett HH. In vivo dynamic imaging of myocardial cell death using 99mTc-labeled C2A domain of synaptotagmin I in a rat model of ischemia and reperfusion. Nucl Med Biol 2007;34:907–915. [PubMed: 17998092]

30. Hofstra L, Liem IH, Dumont EA, Boersma HH, van Heerde WL, Doevendans PA, De Muinck E, Wellens HJ, Kemerink GJ, Reutelingsperger CP, Heidendal GA. Visualisation of cell death in vivo in patients with acute myocardial infarction. Lancet 2000;356:209–212. [PubMed: 10963199]

31. Kietselaer BL, Reutelingsperger CP, Boersma HH, Heidendal GA, Liem IH, Crijns HJ, Narula J, Hofstra L. Noninvasive detection of programmed cell loss with 99mTc-labeled annexin A5 in heart failure. J Nucl Med 2007;48:562–567. [PubMed: 17401092]

32. Narula J, Acio ER, Narula N, Samuels LE, Fyfe B, Wood D, Fitzpatrick JM, Raghunath PN, Tomaszewski JE, Kelly C, Steinmetz N, Green A, Tait JF, Leppo J, Blankenberg FG, Jain D, Strauss HW. Annexin-V imaging for noninvasive detection of cardiac allograft rejection. Nat Med 2001;7:1347–1352. [PubMed: 11726976]

33. Sosnovik DE, Schellenberger EA, Nahrendorf M, Novikov MS, Matsui T, Dai G, Reynolds F, Grazette L, Rosenzweig A, Weissleder R, Josephson L. Magnetic resonance imaging of cardiomyocyte apoptosis with a novel magneto-optical nanoparticle. Magn Reson Med 2005;54:718–724. [PubMed: 16086367]
34. Schellenberger EA, Sosnovik D, Weissleder R, Josephson L. Magneto/optical annexin V, a multimodal protein. Bioconjug Chem 2004;15:1062–1067. [PubMed: 15366960]
35. Hiller KH, Waller C, Nahrendorf M, Bauer WR, Jakob PM. Assessment of cardiovascular apoptosis in the isolated rat heart by magnetic resonance molecular imaging. Mol Imaging 2006;5:115–121. [PubMed: 16954025]
36. Kietselaer BL, Reutelingsperger CP, Heidendal GA, Daemen MJ, Mess WH, Hofstra L, Narula J. Noninvasive detection of plaque instability with use of radiolabeled annexin A5 in patients with carotid-artery atherosclerosis. N Engl J Med 2004;350:1472–1473. [PubMed: 15070807]
37. Sarai M, Hartung D, Petrov A, Zhou J, Narula N, Hofstra L, Kolodgie F, Isobe S, Fujimoto S, Vanderheyden JL, Virmani R, Reutelingsperger C, Wong ND, Gupta S, Narula J. Broad and specific caspase inhibitor-induced acute repression of apoptosis in atherosclerotic lesions evaluated by radiolabeled annexin A5 imaging. J Am Coll Cardiol 2007;50:2305–2312. [PubMed: 18068039]
38. Klein C, Nekolla SG, Balbach T, Schnackenburg B, Nagel E, Fleck E, Schwaiger M. The influence of myocardial blood flow and volume of distribution on late Gd-DTPA kinetics in ischemic heart failure. J Magn Reson Imaging 2004;20:588–593. [PubMed: 15390232]
39. Caravan P, Das B, Dumas S, Epstein FH, Helm PA, Jacques V, Koerner S, Kolodziej A, Shen L, Sun W-C, Zhang Z. Collagen-targeted MRI contrast agent for molecular imaging of fibrosis. Angew Chem Int Ed Engl 2007;46:8171–8173. [PubMed: 17893943]
40. Helm PA, Caravan P, French BA, Jacques V, Shen L, Xu Y, Beyers RJ, Roy RJ, Kramer CM, Epstein FH. Postinfarction myocardial scarring in mice: molecular MR imaging with use of a collagen-targeting contrast agent. Radiology 2008;247:788–796. [PubMed: 18403626]
41. Narula J, Petrov A, Bianchi C, Ditlow CC, Lister BC, Dilley J, Pieslak I, Chen FW, Torchilin VP, Khaw BA. Noninvasive localization of experimental atherosclerotic lesions with mouse/human chimeric Z2D3 F(ab′)2 specific for the proliferating smooth muscle cells of human atheroma. Imaging with conventional and negative charge-modified antibody fragments. Circulation 1995;92:474–484. [PubMed: 7634463]
42. Narula J, Strauss HW. Predicting the likelihood of postangioplastic restenosis: a proliferating challenge for nuclear medicine. J Nucl Med 2000;41:1541–1544. [PubMed: 10994736]
43. Johnson LL, Schofield LM, Verdesca SA, Sharaf BL, Jones RM, Virmani R, Khaw BA. In vivo uptake of radiolabeled antibody to proliferating smooth muscle cells in a swine model of coronary stent restenosis. J Nucl Med 2000;41:1535–1540. [PubMed: 10994735]
44. Shattil SJ. Function and regulation of the beta 3 integrins in hemostasis and vascular biology. Thromb Haemost 1995;74:149–155. [PubMed: 8578448]
45. Murphy JF, Bordet JC, Wyler B, Rissoan MC, Chomarat P, Defrance T, Miossec P, McGregor JL. The vitronectin receptor (alpha v beta 3) is implicated, in cooperation with P-selectin and platelet-activating factor, in the adhesion of monocytes to activated endothelial cells. Biochem J 1994;304:537–542. [PubMed: 7528011]
46. Huang S, Endo RI, Nemerow GR. Upregulation of integrins alpha v beta 3 and alpha v beta 5 on human monocytes and T lymphocytes facilitates adenovirus-mediated gene delivery. J Virol 1995;69:2257–2263. [PubMed: 7533853]
47. Sadeghi MM, Krassilnikova S, Zhang J, Gharaei AA, Fassaei HR, Esmailzadeh L, Kooshkabadi A, Edwards S, Yalamanchili P, Harris TD, Sinusas AJ, Zaret BL, Bender JR. Detection of injury-induced vascular remodeling by targeting activated alphavbeta3 integrin in vivo. Circulation 2004;110:84–90. [PubMed: 15210600]
48. Zhang J, Krassilnikova S, Gharaei AA, Fassaei HR, Esmailzadeh L, Asadi A, Edwards DS, Harris TD, Azure M, Tellides G, Sinusas AJ, Zaret BL, Bender JR, Sadeghi MM. Alphavbeta3-targeted detection of arteriopathy in transplanted human coronary arteries: an autoradiographic study. Faseb J 2005;19:1857–1859. [PubMed: 16150802]

49. Cyrus T, Zhang H, Allen JS, Williams TA, Hu G, Caruthers SD, Wickline SA, Lanza GM. Intramural delivery of rapamycin with alphavbeta3-targeted paramagnetic nanoparticles inhibits stenosis after balloon injury. Arterioscler Thromb Vasc Biol 2008;28:820–826. [PubMed: 18292395]
50. Schafers M, Riemann B, Kopka K, Breyholz HJ, Wagner S, Schafers KP, Law MP, Schober O, Levkau B. Scintigraphic imaging of matrix metalloproteinase activity in the arterial wall in vivo. Circulation 2004;109:2554–2559. [PubMed: 15123523]
51. Zhang J, Nie L, Razavian M, Ahmed M, Dobrucki LW, Asadi A, Edwards DS, Azure M, Sinusas AJ, Sadeghi MM. Molecular imaging of activated matrix metalloproteinases in vascular remodeling. Circulation 2008;118:1953–1960. [PubMed: 18936327]
52. Folkman J. The role of angiogenesis in tumor growth. Semin Cancer Biol 1992;3:65–71. [PubMed: 1378311]
53. Carmeliet P. Angiogenesis in health and disease. Nat Med 2003;9:653–660. [PubMed: 12778163]
54. Kim S, Bell K, Mousa SA, Varner JA. Regulation of angiogenesis in vivo by ligation of integrin alpha5beta1 with the central cell-binding domain of fibronectin. Am J Pathol 2000;156:1345–1362. [PubMed: 10751360]
55. Brooks PC, Clark RA, Cheresh DA. Requirement of vascular integrin alpha v beta 3 for angiogenesis. Science 1994;264:569–571. [PubMed: 7512751]
56. Meoli DF, Sadeghi MM, Krassilnikova S, Bourke BN, Giordano FJ, Dione DP, Su H, Edwards DS, Liu S, Harris TD, Madri JA, Zaret BL, Sinusas AJ. Noninvasive imaging of myocardial angiogenesis following experimental myocardial infarction. J Clin Invest 2004;113:1684–1691. [PubMed: 15199403]
57. Makowski MR, Ebersberger U, Nekolla S, Schwaiger M. In vivo molecular imaging of angiogenesis, targeting alphavbeta3 integrin expression, in a patient after acute myocardial infarction. Eur Heart J 2008;29:2201. [PubMed: 18375397]
58. Hua J, Dobrucki LW, Sadeghi MM, Zhang J, Bourke BN, Cavaliere P, Song J, Chow C, Jahanshad N, van Royen N, Buschmann I, Madri JA, Mendizabal M, Sinusas AJ. Noninvasive imaging of angiogenesis with a 99mTc-labeled peptide targeted at alphavbeta3 integrin after murine hindlimb ischemia. Circulation 2005;111:3255–3260. [PubMed: 15956134]
59. Leong-Poi H, Christiansen J, Heppner P, Lewis CW, Klibanov AL, Kaul S, Lindner JR. Assessment of endogenous and therapeutic arteriogenesis by contrast ultrasound molecular imaging of integrin expression. Circulation 2005;111:3248–3254. [PubMed: 15956135]
60. Winter PM, Morawski AM, Caruthers SD, Fuhrhop RW, Zhang H, Williams TA, Allen JS, Lacy EK, Robertson JD, Lanza GM, Wickline SA. Molecular imaging of angiogenesis in early-stage atherosclerosis with alpha(v)beta3-integrin-targeted nanoparticles. Circulation 2003;108:2270–2274. [PubMed: 14557370]
61. Lu E, Wagner WR, Schellenberger U, Abraham JA, Klibanov AL, Woulfe SR, Csikari MM, Fischer D, Schreiner GF, Brandenburger GH, Villanueva FS. Targeted in vivo labeling of receptors for vascular endothelial growth factor: approach to identification of ischemic tissue. Circulation 2003;108:97–103. [PubMed: 12821549]
62. Rodriguez-Porcel M, Cai W, Gheysens O, Willmann JK, Chen K, Wang H, Chen IY, He L, Wu JC, Li ZB, Mohamedali KA, Kim S, Rosenblum MG, Chen X, Gambhir SS. Imaging of VEGF receptor in a rat myocardial infarction model using PET. J Nucl Med 2008;49:667–673. [PubMed: 18375924]
63. Egami K, Murohara T, Aoki M, Matsuishi T. Ischemia-induced angiogenesis: role of inflammatory response mediated by P-selectin. J Leukoc Biol 2006;79:971–976. [PubMed: 16641139]
64. Heil M, Ziegelhoeffer T, Wagner S, Fernandez B, Helisch A, Martin S, Tribulova S, Kuziel WA, Bachmann G, Schaper W. Collateral artery growth (arteriogenesis) after experimental arterial occlusion is impaired in mice lacking CC-chemokine receptor-2. Circ Res 2004;94:671–677. [PubMed: 14963007]
65. Behm CZ, Kaufmann BA, Carr C, Lankford M, Sanders JM, Rose CE, Kaul S, Lindner JR. Molecular imaging of endothelial vascular cell adhesion molecule-1 expression and inflammatory cell recruitment during vasculogenesis and ischemia-mediated arteriogenesis. Circulation 2008;117:2902–2911. [PubMed: 18506006]

66. Deguchi JO, Aikawa M, Tung CH, Aikawa E, Kim DE, Ntziachristos V, Weissleder R, Libby P. Inflammation in atherosclerosis: visualizing matrix metalloproteinase action in macrophages in vivo. Circulation 2006;114:55–62. [PubMed: 16801460]

67. Su H, Spinale FG, Dobrucki LW, Song J, Hua J, Sweterlitsch S, Dione DP, Cavaliere P, Chow C, Bourke BN, Hu XY, Azure M, Yalamanchili P, Liu R, Cheesman EH, Robinson S, Edwards DS, Sinusas AJ. Non-invasive targeted imaging of matrix metalloproteinase activation in a murine model of postinfarction remodeling. Circulation 2005;112:3157–3167. [PubMed: 16275862]

68. Libby P. Inflammation in atherosclerosis. Nature 2002;420:868–874. [PubMed: 12490960]

69. Trivedi RA, Mallawarachi C, UK-I JM, Graves MJ, Horsley J, Goddard MJ, Brown A, Wang L, Kirkpatrick PJ, Brown J, Gillard JH. Identifying inflamed carotid plaques using in vivo USPIO-enhanced MR imaging to label plaque macrophages. Arterioscler Thromb Vasc Biol 2006;26:1601–1606. [PubMed: 16627809]

70. Nahrendorf M, Zhang H, Hembrador S, Panizzi P, Sosnovik DE, Aikawa E, Libby P, Swirski FK, Weissleder R. Nanoparticle PET-CT imaging of macrophages in inflammatory atherosclerosis. Circulation 2008;117:379–387. [PubMed: 18158358]

71. Amirbekian V, Lipinski MJ, Briley-Saebo KC, Amirbekian S, Aguinaldo JG, Weinreb DB, Vucic E, Frias JC, Hyafil F, Mani V, Fisher EA, Fayad ZA. Detecting and assessing macrophages in vivo to evaluate atherosclerosis noninvasively using molecular MRI. Proc Natl Acad Sci USA 2007;104:961–966. [PubMed: 17215360]

72. Briley-Saebo KC, Shaw PX, Mulder WJ, Choi SH, Vucic E, Aguinaldo JG, Witztum JL, Fuster V, Tsimikas S, Fayad ZA. Targeted molecular probes for imaging atherosclerotic lesions with magnetic resonance using antibodies that recognize oxidation-specific epitopes. Circulation 2008;117:3206–3215. [PubMed: 18541740]

73. Cormode DP, Briley-Saebo KC, Mulder WJ, Aguinaldo JG, Barazza A, Ma Y, Fisher EA, Fayad ZA. An ApoA-I mimetic peptide high-density-lipoprotein-based MRI contrast agent for atherosclerotic plaque composition detection. Small 2008;4:1437–1444. [PubMed: 18712752]

74. Cormode DP, Skajaa T, van Schooneveld MM, Koole R, Jarzyna P, Lobatto ME, Calcagno C, Barazza A, Gordon RE, Zanzonico P, Fisher EA, Fayad ZA, Mulder WJ. Nanocrystal core high-density lipoproteins: a multimodality contrast agent platform. Nano Lett 2008;8:3715–3723. [PubMed: 18939808]

75. Hyafil F, Cornily JC, Feig JE, Gordon R, Vucic E, Amirbekian V, Fisher EA, Fuster V, Feldman LJ, Fayad ZA. Noninvasive detection of macrophages using a nanoparticulate contrast agent for computed tomography. Nat Med 2007;13:636–641. [PubMed: 17417649]

76. Tawakol A, Migrino RQ, Bashian GG, Bedri S, Vermylen D, Cury RC, Yates D, LaMuraglia GM, Furie K, Houser S, Gewirtz H, Muller JE, Brady TJ, Fischman AJ. In vivo 18F-fluorodeoxyglucose positron emission tomography imaging provides a noninvasive measure of carotid plaque inflammation in patients. J Am Coll Cardiol 2006;48:1818–1824. [PubMed: 17084256]

77. Izquierdo-Garcia D, Davies JR, Graves MJ, Rudd JH, Gillard JH, Weissberg PL, Fryer TD, Warburton EA. Comparison of methods for magnetic resonance-guided [18-F]fluorodeoxyglucose positron emission tomography in human carotid arteries. Reproducibility, partial volume correction, and correlation between methods. Stroke. 2008[epub ahead of print]

78. Rudd JH, Myers KS, Bansilal S, Machac J, Pinto CA, Tong C, Rafique A, Hargeaves R, Farkouh M, Fuster V, Fayad ZA. Atherosclerosis inflammation imaging with 18F-FDG PET: carotid, iliac, and femoral uptake reproducibility, quantification methods, and recommendations. J Nucl Med 2008;49:871–878. [PubMed: 18483100]

79. Rudd JH, Myers KS, Bansilal S, Machac J, Rafique A, Farkouh M, Fuster V, Fayad ZA. (18) Fluorodeoxyglucose positron emission tomography imaging of atherosclerotic plaque inflammation is highly reproducible: implications for atherosclerosis therapy trials. J Am Coll Cardiol 2007;50:892–896. [PubMed: 17719477]

80. Nahrendorf M, Jaffer FA, Kelly KA, Sosnovik DE, Aikawa E, Libby P, Weissleder R. Noninvasive vascular cell adhesion molecule-1 imaging identifies inflammatory activation of cells in atherosclerosis. Circulation 2006;114:1504–1511. [PubMed: 17000904]

81. Jaffer FA, Vinegoni C, John MC, Aikawa E, Gold HK, Finn AV, Ntziachristos V, Libby P, Weissleder R. Real-time catheter molecular sensing of inflammation in proteolytically active atherosclerosis. Circulation 2008;118:1802–1809. [PubMed: 18852366]

82. Winter PM, Neubauer AM, Caruthers SD, Harris TD, Robertson JD, Williams TA, Schmieder AH, Hu G, Allen JS, Lacy EK, Zhang H, Wickline SA, Lanza GM. Endothelial alpha(v)beta3 integrin-targeted fumagillin nanoparticles inhibit angiogenesis in atherosclerosis. Arterioscler Thromb Vasc Biol 2006;26:2103–2109. [PubMed: 16825592]
83. Kajstura J, Cheng W, Reiss K, Clark WA, Sonnenblick EH, Krajewski S, Reed JC, Olivetti G, Anversa P. Apoptotic and necrotic myocyte cell deaths are independent contributing variables of infarct size in rats. Lab Invest 1996;74:86–107. [PubMed: 8569201]
84. Khaw BA, Gold HK, Yasuda T, Leinbach RC, Kanke M, Fallon JT, Barlai-Kovach M, Strauss HW, Sheehan F, Haber E. Scintigraphic quantification of myocardial necrosis in patients after intravenous injection of myosin-specific antibody. Circulation 1986;74:501–508. [PubMed: 3017604]
85. Weissleder R, Lee AS, Khaw BA, Shen T, Brady TJ. Antimyosin-labeled monocrystalline iron oxide allows detection of myocardial infarct: MR antibody imaging. Radiology 1992;182:381–385. [PubMed: 1732953]
86. Dec GW, Palacios I, Yasuda T, Fallon JT, Khaw BA, Strauss HW, Haber E. Antimyosin antibody cardiac imaging: its role in the diagnosis of myocarditis. J Am Coll Cardiol 1990;16:97–104. [PubMed: 2358612]
87. Kaufmann BA, Lewis C, Xie A, Mirza-Mohd A, Lindner JR. Detection of recent myocardial ischaemia by molecular imaging of P-selectin with targeted contrast echocardiography. Eur Heart J 2007;28:2011–2017. [PubMed: 17526905]
88. Villanueva FS, Lu E, Bowry S, Kilic S, Tom E, Wang J, Gretton J, Pacella JJ, Wagner WR. Myocardial ischemic memory imaging with molecular echocardiography. Circulation 2007;115:345–352. [PubMed: 17210843]
89. Riou LM, Ruiz M, Sullivan GW, Linden J, Leong-Poi H, Lindner JR, Harris TD, Beller GA, Glover DK. Assessment of myocardial inflammation produced by experimental coronary occlusion and reperfusion with 99mTc-RP517, a new leukotriene B4 receptor antagonist that preferentially labels neutrophils in vivo. Circulation 2002;106:592–598. [PubMed: 12147542]
90. Sosnovik DE, Nahrendorf M, Deliolanis N, Novikov M, Aikawa E, Josephson L, Rosenzweig A, Weissleder R, Ntziachristos V. Fluorescence tomography and magnetic resonance imaging of myocardial macrophage infiltration in infarcted myocardium in vivo. Circulation 2007;115:1384–1391. [PubMed: 17339546]
91. Farrar CT, Dai G, Novikov M, Rosenzweig A, Weissleder R, Rosen BR, Sosnovik DE. Impact of field strength and iron oxide nanoparticle concentration on the linearity and diagnostic accuracy of off-resonance imaging. NMR Biomed 2008;21:453–463. [PubMed: 17918777]
92. Sutton MG, Sharpe N. Left ventricular remodeling after myocardial infarction: pathophysiology and therapy. Circulation 2000;101:2981–2988. [PubMed: 10869273]
93. Nahrendorf M, Sosnovik D, Chen JW, Panizzi P, Figueiredo JL, Aikawa E, Libby P, Swirski FK, Weissleder R. Activatable magnetic resonance imaging agent reports myeloperoxidase activity in healing infarcts and noninvasively detects the antiinflammatory effects of atorvastatin on ischemia-reperfusion injury. Circulation 2008;117:1153–1160. [PubMed: 18268141]
94. Heymans S, Luttun A, Nuyens D, Theilmeier G, Creemers E, Moons L, Dyspersin GD, Cleutjens JP, Shipley M, Angellilo A, Levi M, Nube O, Baker A, Keshet E, Lupu F, Herbert JM, Smits JF, Shapiro SD, Baes M, Borgers M, Collen D, Daemen MJ, Carmeliet P. Inhibition of plasminogen activators or matrix metalloproteinases prevents cardiac rupture but impairs therapeutic angiogenesis and causes cardiac failure. Nat Med 1999;5:1135–1142. [PubMed: 10502816]
95. Nahrendorf M, Hu K, Frantz S, Jaffer FA, Tung CH, Hiller KH, Voll S, Nordbeck P, Sosnovik D, Gattenlohner S, Novikov M, Dickneite G, Reed GL, Jakob P, Rosenzweig A, Bauer WR, Weissleder R, Ertl G. Factor XIII deficiency causes cardiac rupture, impairs wound healing, and aggravates cardiac remodeling in mice with myocardial infarction. Circulation 2006;113:1196–1202. [PubMed: 16505171]
96. Gemmati D, Federici F, Campo G, Tognazzo S, Serino ML, De Mattei M, Valgimigli M, Malagutti P, Guardigli G, Ferraresi P, Bernardi F, Ferrari R, Scapoli GL, Catozzi L. Factor XIIIA-V34L and factor XIIIB-H95R gene variants: effects on survival in myocardial infarction patients. Mol Med 2007;13:112–120. [PubMed: 17515963]
97. Nahrendorf M, Aikawa E, Figueiredo JL, Stangenberg L, van den Borne SW, Blankesteijn WM, Sosnovik DE, Jaffer FA, Tung CH, Weissleder R. Transglutaminase activity in acute infarcts predicts

healing outcome and left ventricular remodelling: implications for FXIII therapy and anti-thrombin use in myocardial infarction. Eur Heart J 2008;29:445–454. [PubMed: 18276618]

98. Shirani J, Dilsizian V. Imaging left ventricular remodeling: targeting the neurohumoral axis. Nat Clin Pract Cardiovasc Med 2008;5:S57–S62. [PubMed: 18641608]
99. Knuefermann P, Vallejo J, Mann DL. The role of innate immune responses in the heart in health and disease. Trends Cardiovasc Med 2004;14:1–7. [PubMed: 14720467]
100. Tillmanns J, Carlsen H, Blomhoff R, Valen G, Calvillo L, Ertl G, Bauersachs J, Frantz S. Caught in the act: in vivo molecular imaging of the transcription factor NF-kappaB after myocardial infarction. Biochem Biophys Res Commun 2006;342:773–774. [PubMed: 16497270]
101. Cohn JN, Levine TB, Olivari MT, Garberg V, Lura D, Francis GS, Simon AB, Rector T. Plasma norepinephrine as a guide to prognosis in patients with chronic congestive heart failure. N Engl J Med 1984;311:819–823. [PubMed: 6382011]
102. Frist W, Yasuda T, Segall G, Khaw BA, Strauss HW, Gold H, Stinson E, Oyer P, Baldwin J, Billingham M, McDougall R, Haber E. Noninvasive detection of human cardiac transplant rejection with indium-111 antimyosin (Fab) imaging. Circulation 1987;76:V81–V85. [PubMed: 3311460]
103. Kanno S, Wu YJ, Lee PC, Dodd SJ, Williams M, Griffith BP, Ho C. Macrophage accumulation associated with rat cardiac allograft rejection detected by magnetic resonance imaging with ultrasmall superparamagnetic iron oxide particles. Circulation 2001;104:934–938. [PubMed: 11514382]
104. Wu YL, Ye Q, Foley LM, Hitchens TK, Sato K, Williams JB, Ho C. In situ labeling of immune cells with iron oxide particles: an approach to detect organ rejection by cellular MRI. Proc Natl Acad Sci USA 2006;103:1852–1857. [PubMed: 16443687]
105. Tanaka M, Swijnenburg RJ, Gunawan F, Cao YA, Yang Y, Caffarelli AD, de Bruin JL, Contag CH, Robbins RC. In vivo visualization of cardiac allograft rejection and trafficking passenger leukocytes using bioluminescence imaging. Circulation 2005;112:I105–I110. [PubMed: 16159800]
106. Weller GE, Lu E, Csikari MM, Klibanov AL, Fischer D, Wagner WR, Villanueva FS. Ultrasound imaging of acute cardiac transplant rejection with microbubbles targeted to intercellular adhesion molecule-1. Circulation 2003;108:218–224. [PubMed: 12835214]
107. Arbab AS, Yocum GT, Rad AM, Khakoo AY, Fellowes V, Read EJ, Frank JA. Labeling of cells with ferumoxidesprotamine sulfate complexes does not inhibit function or differentiation capacity of hematopoietic or mesenchymal stem cells. NMR Biomed 2005;18:553–559. [PubMed: 16229060]
108. Kostura L, Kraitchman DL, Mackay AM, Pittenger MF, Bulte JW. Feridex labeling of mesenchymal stem cells inhibits chondrogenesis but not adipogenesis or osteogenesis. NMR Biomed 2004;17:513–517. [PubMed: 15526348]
109. Frank JA, Miller BR, Arbab AS, Zywicke HA, Jordan EK, Lewis BK, Bryant LH Jr, Bulte JW. Clinically applicable labeling of mammalian and stem cells by combining superparamagnetic iron oxides and transfection agents. Radiology 2003;228:480–487. [PubMed: 12819345]
110. Walczak P, Kedziorek DA, Gilad AA, Lin S, Bulte JW. Instant MR labeling of stem cells using magnetoelectroporation. Magn Reson Med 2005;54:769–774. [PubMed: 16161115]
111. Hill JM, Dick AJ, Raman VK, Thompson RB, Yu ZX, Hinds KA, Pessanha BS, Guttman MA, Varney TR, Martin BJ, Dunbar CE, McVeigh ER, Lederman RJ. Serial cardiac magnetic resonance imaging of injected mesenchymal stem cells. Circulation 2003;108:1009–1014. [PubMed: 12912822]
112. Kraitchman DL, Heldman AW, Atalar E, Amado LC, Martin BJ, Pittenger MF, Hare JM, Bulte JW. In vivo magnetic resonance imaging of mesenchymal stem cells in myocardial infarction. Circulation 2003;107:2290–2293. [PubMed: 12732608]
113. Amsalem Y, Mardor Y, Feinberg MS, Landa N, Miller L, Daniels D, Ocherashvilli A, Holbova R, Yosef O, Barbash IM, Leor J. Iron-oxide labeling and outcome of transplanted mesenchymal stem cells in the infarcted myocardium. Circulation 2007;116:I38–I45. [PubMed: 17846324]
114. Stuckey DJ, Carr CA, Martin-Rendon E, Tyler DJ, Willmott C, Cassidy PJ, Hale SJ, Schneider JE, Tatton L, Harding SE, Radda GK, Watt S, Clarke K. Iron particles for noninvasive monitoring of bone marrow stromal cell engraftment into, and isolation of viable engrafted donor cells from, the heart. Stem Cells 2006;24:1968–1975. [PubMed: 16627684]

115. Partlow KC, Chen J, Brant JA, Neubauer AM, Meyerrose TE, Creer MH, Nolta JA, Caruthers SD, Lanza GM, Wickline SA. 19F magnetic resonance imaging for stem/progenitor cell tracking with multiple unique perfluorocarbon nanobeacons. Faseb J 2007;21:1647–1654. [PubMed: 17284484]
116. Walczak P, Kedziorek DA, Gilad AA, Barnett BP, Bulte JW. Applicability and limitations of MR tracking of neural stem cells with asymmetric cell division and rapid turnover: the case of the shiverer dysmyelinated mouse brain. Magn Reson Med 2007;58:261–269. [PubMed: 17654572]
117. Bulte JW, Kraitchman DL. Monitoring cell therapy using iron oxide MR contrast agents. Curr Pharm Biotechnol 2004;5:567–584. [PubMed: 15579045]
118. Kraitchman DL, Tatsumi M, Gilson WD, Ishimori T, Kedziorek D, Walczak P, Segars WP, Chen HH, Fritzges D, Izbudak I, Young RG, Marcelino M, Pittenger MF, Solaiyappan M, Boston RC, Tsui BM, Wahl RL, Bulte JW. Dynamic imaging of allogeneic mesenchymal stem cells trafficking to myocardial infarction. Circulation 2005;112:1451–1461. [PubMed: 16129797]
119. Terrovitis JV, Bulte JW, Sarvananthan S, Crowe LA, Sarathchandra P, Batten P, Sachlos E, Chester AH, Czernuszka JT, Firmin DN, Taylor PM, Yacoub MH. Magnetic resonance imaging of ferumoxide-labeled mesenchymal stem cells seeded on collagen scaffolds-relevance to tissue engineering. Tissue Eng 2006;12:2765–2775. [PubMed: 17518646]
120. Barnett BP, Kraitchman DL, Lauzon C, Magee CA, Walczak P, Gilson WD, Arepally A, Bulte JW. Radiopaque alginate microcapsules for X-ray visualization and immunoprotection of cellular therapeutics. Mol Pharm 2006;3:531–538. [PubMed: 17009852]
121. Zhang SJ, Wu JC. Comparison of imaging techniques for tracking cardiac stem cell therapy. J Nucl Med 2007;48:1916–1919. [PubMed: 18056330]
122. Cao F, Drukker M, Lin S, Sheikh AY, Xie X, Li Z, Connolly AJ, Weissman IL, Wu JC. Molecular imaging of embryonic stem cell misbehavior and suicide gene ablation. Cloning Stem Cells 2007;9:107–117. [PubMed: 17386018]
123. van der Bogt KE, Sheikh AY, Schrepfer S, Hoyt G, Cao F, Ransohoff KJ, Swijnenburg RJ, Pearl J, Lee A, Fischbein M, Contag CH, Robbins RC, Wu JC. Comparison of different adult stem cell types for treatment of myocardial ischemia. Circulation 2008;118:S121–S129. [PubMed: 18824743]
124. Terrovitis J, Stuber M, Youssef A, Preece S, Leppo M, Kizana E, Schar M, Gerstenblith G, Weiss RG, Marban E, Abraham MR. Magnetic resonance imaging overestimates ferumoxide-labeled stem cell survival after transplantation in the heart. Circulation 2008;117:1555–1562. [PubMed: 18332264]
125. Cao F, Lin S, Xie X, Ray P, Patel M, Zhang X, Drukker M, Dylla SJ, Connolly AJ, Chen X, Weissman IL, Gambhir SS, Wu JC. In vivo visualization of embryonic stem cell survival, proliferation, and migration after cardiac delivery. Circulation 2006;113:1005–1014. [PubMed: 16476845]
126. Gyongyosi M, Blanco J, Marian T, Tron L, Petnehazy O, Petrasi Z, Hemetsberger R, Rodriquez J, Font G, Pavo GF, Kertesz I, Balkay L, Pavo N, Posa A, Emri M, Galuska L, Kraitchman DL, Wojta J, Huber K, Glogar D. Serial noninvasive in vivo positron emission tomographic (PET) tracking of percutaneously intramyocardially injected autologous porcine mesenchymal stem cells modified for transgene reporter gene expression. Circ Cardiovasc Imaging 2008;1:94–103. [PubMed: 19808526]
127. Bengel FM, Anton M, Richter T, Simoes MV, Haubner R, Henke J, Erhardt W, Reder S, Lehner T, Brandau W, Boekstegers P, Nekolla SG, Gansbacher B, Schwaiger M. Noninvasive imaging of transgene expression by use of positron emission tomography in a pig model of myocardial gene transfer. Circulation 2003;108:2127–2133. [PubMed: 14530205]
128. Rodriguez-Porcel M, Brinton TJ, Chen IY, Gheysens O, Lyons J, Ikeno F, Willmann JK, Wu L, Wu JC, Yeung AC, Yock P, Gambhir SS. Reporter gene imaging following percutaneous delivery in swine moving toward clinical applications. J Am Coll Cardiol 2008;51:595–597. [PubMed: 18237691]
129. Yaghoubi S, Jensen MC, Satyamurthy N, Budhiraja S, Paik D, Czernin J, Gambhir SS. Noninvasive detection of therapeutic cytolytic T cells with [18F]FHBG positron emission tomography in a glioma patient. Nat Clin Pract Oncol. 2008epub ahead of print
130. Avril N, Bengel FM. Defining the success of cardiac gene therapy: how can nuclear imaging contribute? Eur J Nucl Med Mol Imaging 2003;30:757–771. [PubMed: 12541135]

131. Wu JC, Inubushi M, Sundaresan G, Schelbert HR, Gambhir SS. Positron emission tomography imaging of cardiac reporter gene expression in living rats. Circulation 2002;106:180–183. [PubMed: 12105155]

132. Wu JC, Inubushi M, Sundaresan G, Schelbert HR, Gambhir SS. Optical imaging of cardiac reporter gene expression in living rats. Circulation 2002;105:1631–1634. [PubMed: 11940538]

133. Chen IY, Wu JC, Min JJ, Sundaresan G, Lewis X, Liang Q, Herschman HR, Gambhir SS. Micro-positron emission tomography imaging of cardiac gene expression in rats using bicistronic adenoviral vector-mediated gene delivery. Circulation 2004;109:1415–1420. [PubMed: 15007006]

134. Miyagawa M, Anton M, Wagner B, Haubner R, Souvatzoglou M, Gansbacher B, Schwaiger M, Bengel FM. Noninvasive imaging of cardiac transgene expression with PET: comparison of the human sodium/iodide symporter gene and HSV1-tk as the reporter gene. Eur J Nucl Med Mol Imaging 2005;32:1108–1114. [PubMed: 15988610]

135. Bengel FM, Anton M, Avril N, Brill T, Nguyen N, Haubner R, Gleiter E, Gansbacher B, Schwaiger M. Uptake of radiolabeled 2′-fluoro-2′-deoxy-5-iodo-1-beta-D-arabinofuranosyluracil in cardiac cells after adenoviral transfer of the herpesvirus thymidine kinase gene: the cellular basis for cardiac gene imaging. Circulation 2000;102:948–950. [PubMed: 10961956]

136. Inubushi M, Wu JC, Gambhir SS, Sundaresan G, Satyamurthy N, Namavari M, Yee S, Barrio JR, Stout D, Chatziioannou AF, Wu L, Schelbert HR. Positron-emission tomography reporter gene expression imaging in rat myocardium. Circulation 2003;107:326–332. [PubMed: 12538436]

137. Wu JC, Chen IY, Wang Y, Tseng JR, Chhabra A, Salek M, Min JJ, Fishbein MC, Crystal R, Gambhir SS. Molecular imaging of the kinetics of vascular endothelial growth factor gene expression in ischemic myocardium. Circulation 2004;110:685–691. [PubMed: 15302807]

138. Anton M, Wittermann C, Haubner R, Simoes M, Reder S, Essien B, Wagner B, Henke J, Erhardt W, Noll S, Hackett NR, Crystal RG, Schwaiger M, Gansbacher B, Bengel FM. Coexpression of herpesviral thymidine kinase reporter gene and VEGF gene for noninvasive monitoring of therapeutic gene transfer: an in vitro evaluation. J Nucl Med 2004;45:1743–1746. [PubMed: 15471843]

139. Wagner B, Anton M, Nekolla SG, Reder S, Henke J, Seidl S, Hegenloh R, Miyagawa M, Haubner R, Schwaiger M, Bengel FM. Noninvasive characterization of myocardial molecular interventions by integrated positron emission tomography and computed tomography. J Am Coll Cardiol 2006;48:2107–2115. [PubMed: 17113000]

140. Chang GY, Cao F, Krishnan M, Huang M, Li Z, Xie X, Sheikh AY, Hoyt G, Robbins RC, Hsiai T, Schneider MD, Wu JC. Positron emission tomography imaging of conditional gene activation in the heart. J Mol Cell Cardiol 2007;43:18–26. [PubMed: 17467733]

141. Catana C, Procissi D, Wu Y, Judenhofer MS, Qi J, Pichler BJ, Jacobs RE, Cherry SR. Simultaneous in vivo positron emission tomography and magnetic resonance imaging. Proc Natl Acad Sci USA 2008;105:3705–3710. [PubMed: 18319342]

142. Kooi ME, Cappendijk VC, Cleutjens KB, Kessels AG, Kitslaar PJ, Borgers M, Frederik PM, Daemen MJ, van Engelshoven JM. Accumulation of ultrasmall superparamagnetic particles of iron oxide in human atherosclerotic plaques can be detected by in vivo magnetic resonance imaging. Circulation 2003;107:2453–2458. [PubMed: 12719280]

143. Rudd JH, Warburton EA, Fryer TD, Jones HA, Clark JC, Antoun N, Johnstrom P, Davenport AP, Kirkpatrick PJ, Arch BN, Pickard JD, Weissberg PL. Imaging atherosclerotic plaque inflammation with [18F]-fluorodeoxyglucose positron emission tomography. Circulation 2002;105:2708–2711. [PubMed: 12057982]

144. Harisinghani MG, Barentsz J, Hahn PF, Deserno WM, Tabatabaei S, van de Kaa CH, de la Rosette J, Weissleder R. Noninvasive detection of clinically occult lymph-node metastases in prostate cancer. N Engl J Med 2003;348:2491–2499. [PubMed: 12815134]

145. Spuentrup E, Katoh M, Wiethoff AJ, Buecker A, Botnar RM, Parsons EC, Guenther RW. Molecular coronary MR imaging of human thrombi using EP-2104R, a fibrin-targeted contrast agent: experimental study in a swine model. Rofo 2007;179:1166–1173. [PubMed: 17948194]

146. Calcagno C, Cornily JC, Hyafil F, Rudd JH, Briley-Saebo KC, Mani V, Goldschlager G, Machac J, Fuster V, Fayad ZA. Detection of neovessels in atherosclerotic plaques of rabbits using dynamic contrast enhanced MRI and 18F-FDG PET. Arterioscler Thromb Vasc Biol 2008;28:1311–1317. [PubMed: 18467641]

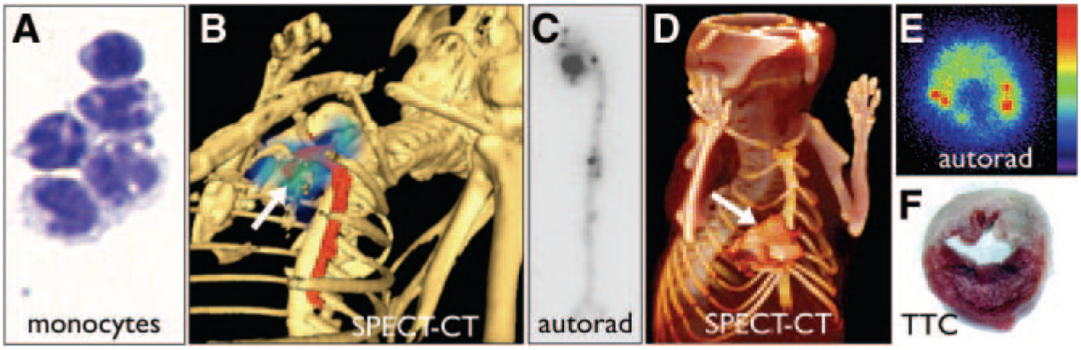

Figure 1.

Inflammation. A, Cytospin of cell-sorted monocytes, adapted from Swirski et al.[11] B, SPECT-CT image after injection of ^{111}In-labeled monocytes that migrated to inflamed atherosclerotic lesions in the aortic root of an apoE$^{-/-}$ mouse (arrow), adapted from Kircher et al.[9] C, Autoradiography of excized aorta after adoptive tranfer of radioactively labeled monocytes shows accumulation in the plaque-rich aortic root.[11] D–F, Adoptive transfer of radioactively labeled Ly6C^{hi} monocytes on day 2 after myocardial infarction.[10] The SPECT/CT image, ex vivo autoradiography, and concomitant 2–3-5-triphenyl tetrazolium chloride staining show accumulation of labeled monocytes in the infarct (M.N. and F.S., unpublished data).

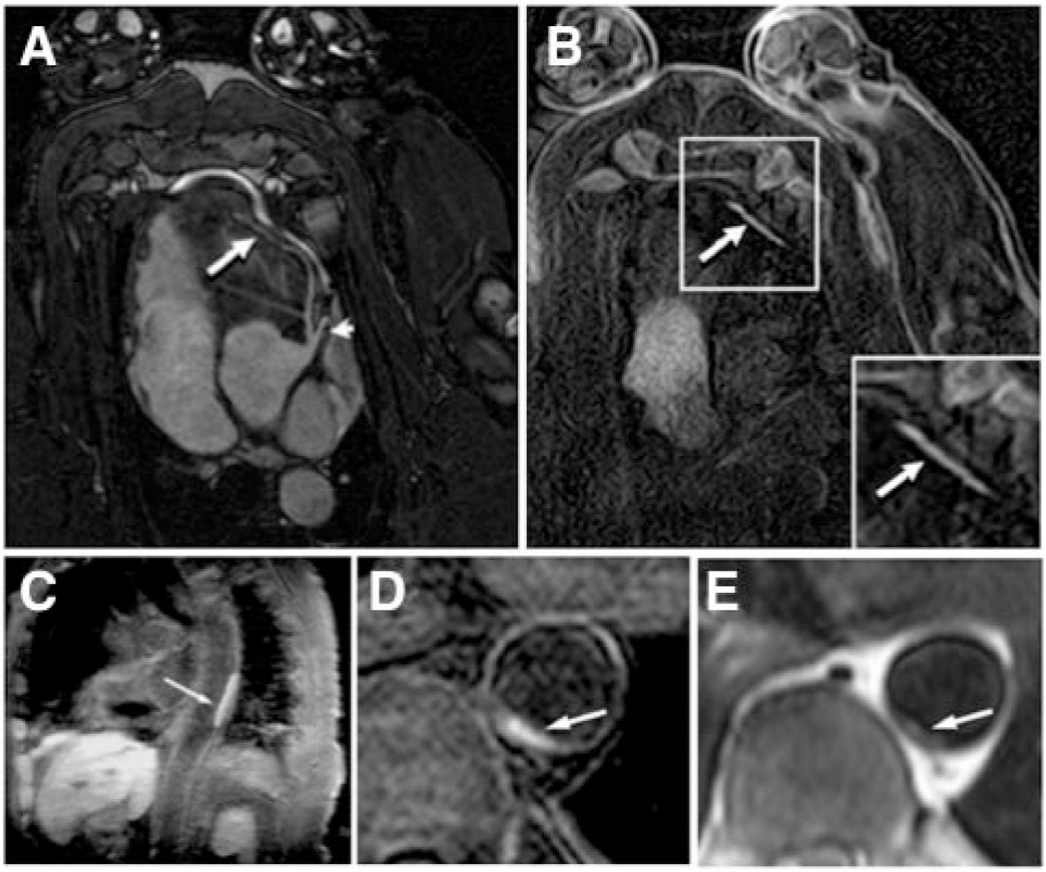

Figure 2.
Thrombosis. A and B, molecular MRI of coronary thrombosis in a swine model using EP-2104R, a fibrin-specific contrast agent. SSFP sequence (A) and IR sequence (B) 2 hours after EP2104R, adapted with permission.[145] C–E, Molecular MRI in patients, adapted with permission.[21] C, Aortic thrombus of an 82-year-old female patient. D and E, Aortic thrombus in the descending thoracic aorta of a 65-year-old male patient using inversion recovery black-blood gradient-echo imaging.

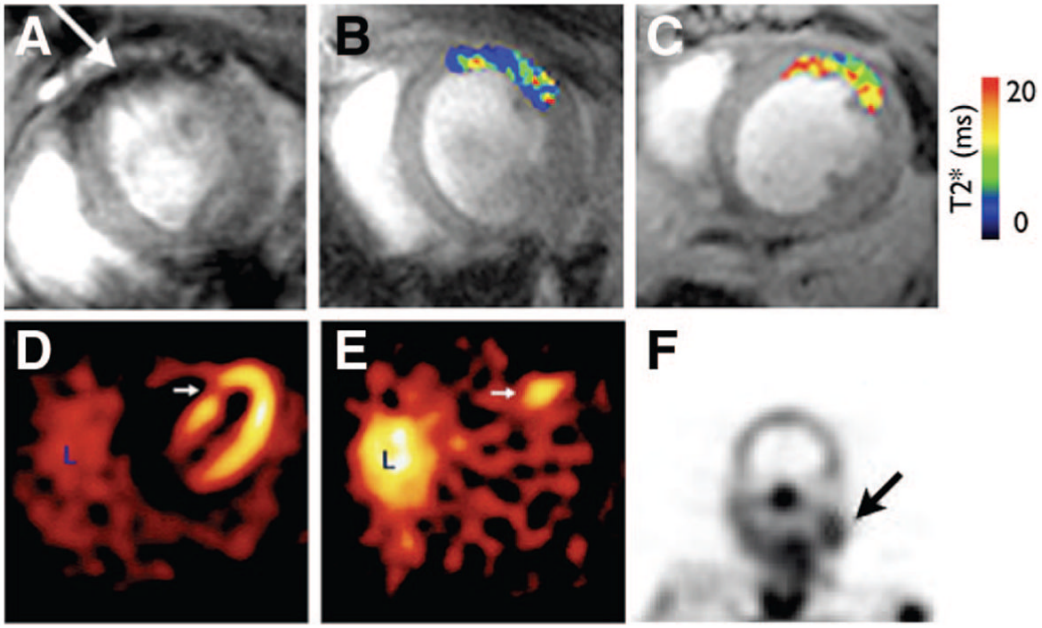

Figure 3.

Apoptosis. A–C, Molecular MRI of CM apoptosis in vivo in a mouse model of ischemia-reperfusion, adapted with permission.[33] A, The apoptosis sensing magnetofluorescent nanoparticle, AnxCLIO-Cy5.5, accumulates in injured myocardium producing signal hypointensity (arrow) and a reduction in T2*. B and C, In vivo T2* maps created in regions of myocardium with equivalent degrees of hypokinesis in a mouse injected with AnxCLIO-Cy5.5 (B) and a mouse injected with the control probe (C). D and E, Imaging of cell death with techenetium-labeled annexin in a patient with an acute coronary syndrome, adapted with permission.[30] D, Perfusion defect (arrow) in the patient 6 to 8 weeks after the acute coronary syndrome. E, Uptake of 99mTc annexin-V (arrow) at the time of the event correlates well with the perfusion defect. L, liver. F, Uptake of 99mTc annexin-V in a patient before carotid endarterectomy. A strong correlation was seen in this study between uptake of the probe and macrophage content of the plaque, adapted with permission.[36]

Figure 4.
Molecular imaging of postinfarct collagen deposition. A, CMR image shows a short-axis slice acquired before contrast. B, After the injection of the collagen-targeted contrast agent (EP-3533). C, Corresponding tissue slice at right shows collagen in red after Picrosirius staining, adapted with permission.[40]

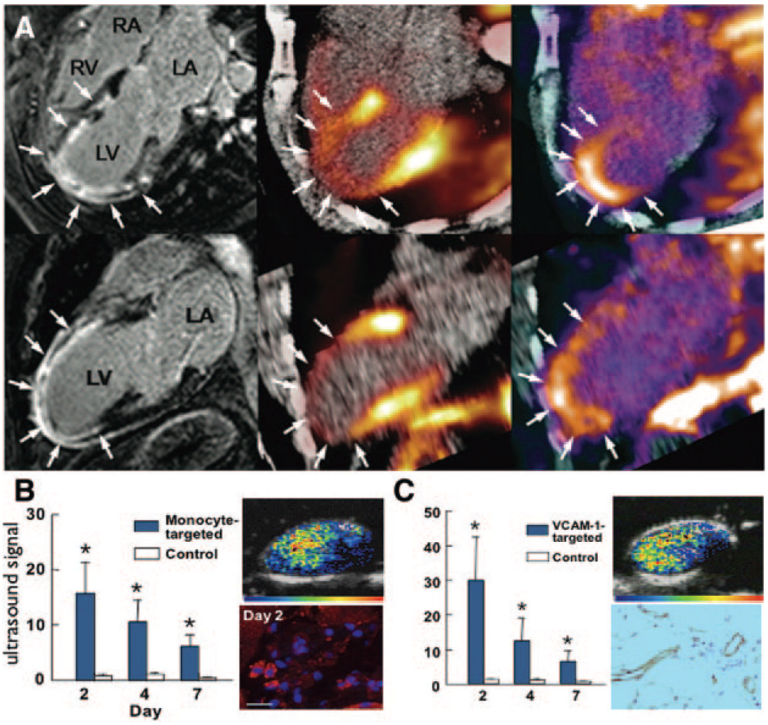

Figure 5.

Angiogenesis imaging. A, Imaging of integrin expression in a patient 2 weeks after acute anterior myocardial infarction. Magnetic resonance images with delayed gadolinium enhancement (left panel) and hybrid PET/CT perfusion imaging with ^{13}N-ammonia (middle) demonstrate a large infarction in the anteroapical segments. PET performed after injection of an 18F-labeled probe targeting integrin by an RGD sequence detected tracer uptake in the infarct region (right), reproduced with permission.[57] B, Ultrasound molecular imaging of inflammation in angiogenesis in mouse ischemic hindlimb. Data are shown for microbubbles targeted to monocytes and VCAM-1 (C). Corresponding examples of molecular imaging with targeted microbubbles at day 2 and immunohistochemistry for monocyte α-integrin (red) and VCAM-1 are shown to the right of each graph. *P <0.05 versus control microbubble signal, reproduced with permission.[65]

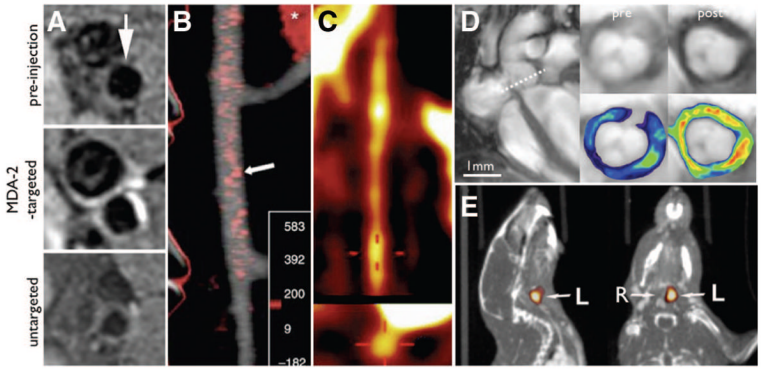

Figure 6.

Atherosclerosis imaging. A, Imaging of inflammatory atherosclerosis in rabbits using Gd-loaded oxLDL-targeted micelles, adapted with permission.[72] B, Macrophage-targeted nanoparticles enable CT imaging of inflammatory atherosclerosis in a rabbit model, adapted with permission.[75] C, FDG PET imaging in a rabbit model of atherosclerosis, adapted with permission.[146] D, MRI of VCAM-1 in the aortic root of apoE$^{-/-}$ mice. After injection of VCAM-1–targeted nanoparticles, a signal decrease was observed on T2* weighted gradient MRI, adapted with permission.[80] E, RP782 MMP-targeted microSPECT-CT 3 weeks after carotid injury in the apoE$^{-/-}$ mouse. Arrows point to the injured left (L) and noninjured right (R) carotid arteries, adapted with permission.[51]

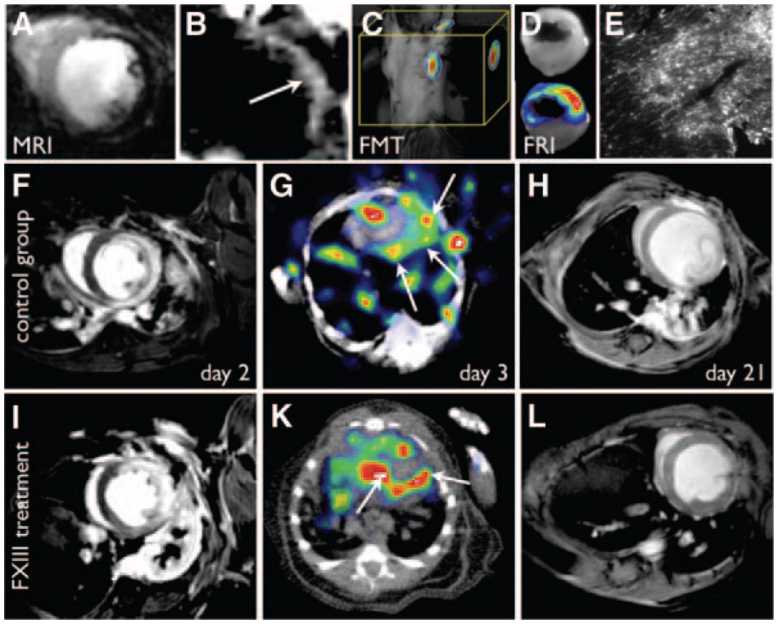

Figure 7.

Ischemia and post-MI remodeling. A–E, Magnetofluorescent imaging of postinfarction myocardial monocyte/macrophage infiltration. A, T2*-weighted MRI, 96 hours after infarction, shows the accumulation of iron oxide nanoparticles in the infarct (signal hypointensity) due to their uptake by infiltrating macrophages, reproduced with permission.[90] B, Off-resonance image in the same animal model as in A producing positive contrast from the iron oxide nanoparticles, reproduced with permission.[91] C, FMT imaging after injection of magnetofluorescent nanoparticles shows high fluorescent signal in the region of the heart (M.N. and Ralph Weissleder, unpublished data). D, Ex vivo fluorescence reflectance imaging confirms in vivo FMT. E, Fluorescent microscopy of the myocardial infarct in the 680-nm channel shows the microscopic distribution of the nanoparticles, reproduced with permission.[90] F–L, Serial MRI and SPECT-CT imaging of infarct healing and left ventricular remodeling. SPECT imaging of FXIII activity in the healing infarct predicts the degree of LV remodeling. F and I, Delayed enhancement MR images on day 2 post-MI show similar infarct size and LV volumes in mice without (F–H) and with (I–L) FXIII therapy. FXIII activity on day 3 is significantly higher in the treated mouse (G, K) and correlates with less adverse remodeling by day 21 post-MI (H, L), adapted with permission.[97]

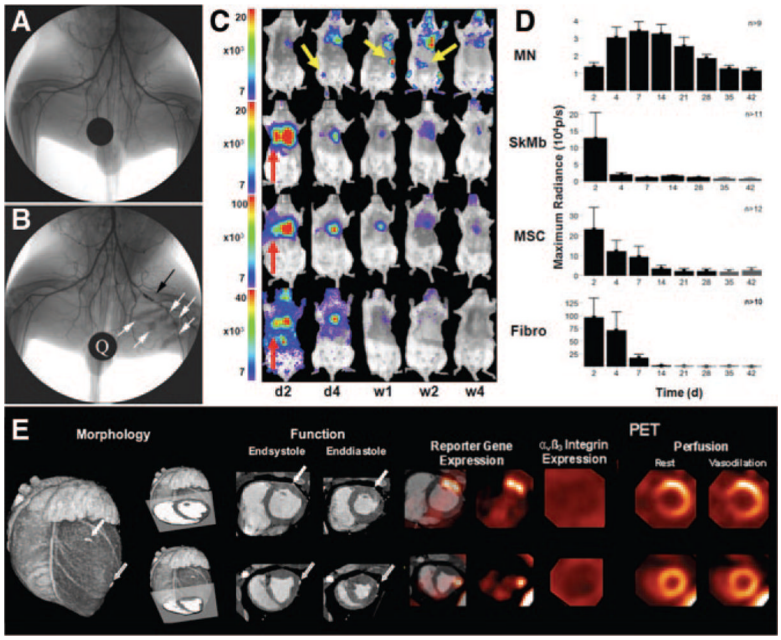

Figure 8.

Cell and gene therapy. A and B, X-ray angiogram of the peripheral hindlimb of a rabbit before intervention (A) and after creation of a femoral artery occlusion via a platinum coil (black arrow). X-ray–visible microencapsulated stem cell injections injected intra-muscularly in the medial thigh appear as radiopacities (B, white arrows). A quarter (Q) is used for reference, adapted with permission.[120] C and D, Comparison of different adult stem cell types for treatment of myocardial ischemia. Bone marrow mononuclear cells (MN), mesenchymal stem cells (MSC), skeletal myoblasts (SkMb), and fibroblasts (Fibro) were isolated from transgenic mice that stably express firefly luciferase and green fluorescence protein and then injected into syngenic FVB mice. BLI from the same representative animal within each group reveals cell proliferation, death, and migration. MN show retention in the heart and can home in on the femur, spleen, and liver (yellow arrows). BLI from animals 2 days after injection of SkMb, MSC, and Fibro show retention not only in the heart but also in the lungs (red arrows). Decreasing signal intensity over time is indicative of acute donor cell death in these groups. Scale bars represent BLI signal in photons/s/cm^2/sr. Quantification of BLI signals (D) on fixed regions of interest (ROI) over the heart reveal an early increase in signal from day 2 until day 7 in the MN group, whereas signal intensity in the SkMb, MSC, and Fibro groups clearly decreases until background signal (black bars) at weeks 3 to 4, reproduced with permission.[123] E, Comprehensive monitoring of myocardial gene transfer by hybrid PET-CT, adapted from Wagner et al[139]. Representative short-axis slices of a healthy pig heart are shown. Using intramyocardial injection of adenoviral vectors, gene transfer was conducted to 2 sites. At the basal site (top), vascular endothelial growth factor was coexpressed with a mutant herpesviral thymidine kinase reporter gene (HSV1-sr39tk). At the distal site, only reporter gene was expressed as control. Imaging was conducted 2 days after gene transfer. Contrast-enhanced CT shows cardiac morphology, clip-marked injection sites, and wall thickness/thickening (left). PET reporter gene imaging confirms successful transgene expression at both sites (middle left). Imaging of $\alpha\beta_3$ integrins using F-18 galactoRGD shows absence of adhesion molecule expression at the early stage of genetic intervention (middle right). Perfusion imaging shows regional increase at site of VEGF coexpression, not at control injection site (right), suggesting VEGF-specific effect on regional perfusion. A single modality was used to characterize the molecular intervention from gene expression over protein expression and physiology to morphology.